Copyright Warning & Restrictions

The copyright law of the United States (Title 17, United States Code) governs the making of photocopies or other reproductions of copyrighted material.

Under certain conditions specified in the law, libraries and archives are authorized to furnish a photocopy or other reproduction. One of these specified conditions is that the photocopy or reproduction is not to be "used for any purpose other than private study, scholarship, or research." If a, user makes a request for, or later uses, a photocopy or reproduction for purposes in excess of "fair use" that user may be liable for copyright infringement,

This institution reserves the right to refuse to accept a copying order if, in its judgment, fulfillment of the order would involve violation of copyright law.

Please Note: The author retains the copyright while the New Jersey Institute of Technology reserves the right to distribute this thesis or dissertation

Printing note: If you do not wish to print this page, then select "Pages from: first page # to: last page #" on the print dialog screen

NJIT New Jersey's Science & Technology University

The Van Houten library has removed some of the personal information and all signatures from the approval page and biographical sketches of theses and dissertations in order to protect the identity of NJIT graduates and faculty.

ABSTRACT

THE IMPACT OF DYNAMIC AND PASSIVE STANDING ON BONE MINERAL DENSITY AND APPOSITIONAL GROWTH IN IMMOBILIZED CHILDREN

by
Megan Diane Damcott

The first discovery of the potential role that mechanical loading has on determining the strength of bone occurred in 1892. However, for almost a century after this discovery, the specific mechanisms influenced by mechanical loading remained locked in a mysterious 'black box'. Then in the 1960s, the 'black box' was opened and continued work has now unlocked the basic mechanisms involved in mechanical loading and whole-bone strength. This increased knowledge has spurred clinicians and researchers to investigate the impact of weight-bearing interventions on individuals with an increased risk of osteoporosis. The most common weight-bearing clinical intervention used in non-ambulant populations is passive standing. However, insurance companies are increasingly denying reimbursement for standers, quoting that there is not enough scientific literature proving the benefits of the intervention. This study continues the investigation of the impact of passive standing, while introducing and investigating the impact of a novel dynamic stander which mimics the walking gait. A fifteen-month study was initiated to determine the impact of each clinical intervention on bone mineral density, bone mineral content and area in non-ambulant children. Dual-energy x-ray absorptiometry (DXA) was used to calculate the aforementioned parameters as it is the current 'gold standard' in the field, though limitations do exist in the calculation of density, content and area in low density populations. Due to these limitations, this study also investigates potential improvements to the algorithms used in DXA to increase the precision of this study and future work.

THE IMPACT OF DYNAMIC AND PASSIVE STANDING ON BONE MINERAL DENSITY AND APPOSITIONAL GROWTH IN IMMOBILIZED CHILDREN

by
Megan Diane Damcott

A Dissertation
Submitted to the Faculty of
New Jersey Institute of Technology
and University of Medicine and Dentistry of New Jersey
in Partial Fulfillment of the Requirements for the Degree of
Doctor of Philosophy in Biomedical Engineering

Joint Program in Biomedical Engineering

August 2011

Copyright © 2011 by Megan Diane Damcott

ALL RIGHTS RESERVED

.

APPROVAL PAGE

THE IMPACT OF DYNAMIC AND PASSIVE STANDING ON BONE MINERAL DENSITY AND APPOSITIONAL GROWTH IN IMMOBILIZED CHILDREN

Megan Diane Damcott

Dr. Richard Foulds, Dissertation Advisor — Date
Associate Professor of Biomedical Engineering, NJIT

Dr. Bryan Pfister, Committee Member — Date
Assistant Professor of Biomedical Engineering, NJIT

Dr. William Van Buskirk, Committee Member — Date
Distinguished Professor and Chair of Biomedical Engineering, NJIT

Dr. Sheldon Lin, Committee Member — Date
Associate Professor of Orthopaedics, UMDNJ

Dr. Christopher Fritton, Committee Member — Date
Assistant Professor of Orthopaedics, UMDNJ

BIOGRAPHICAL SKETCH

Author: Megan Diane Damcott

Degree: Doctor of Philosophy

Date: May 2011

Undergraduate and Graduate Education:

- Doctor of Philosophy in Biomedical Engineering,
  New Jersey Institute of Technology, Newark, NJ,
  University of Medicine and Dentistry of New Jersey, Newark, NJ, 2011

- Master of Science in Biomedical Engineering,
  New Jersey Institute of Technology, Newark, NJ, 2011

- Bachelor of Science in Biomedical Engineering,
  University of Rochester, Rochester, NY 2005

Major: Biomedical Engineering

Presentations and Publications:

Damcott, M. "The Effect of Dynamic Standing on the Bone Mineral Density of Non-Ambulatory Children: A Pilot Study." Master's Thesis, New Jersey Institute of Technology: May 2011.

Lieberman B, Alqumeran M, Scharf J, Damcott M, Foulds R. "Design of an Assistive Eating Utensil for an Individual with Arthrogryposis Multiplex Congenital." Proceedings and Poster Presentation 36th Annual Northeast Bioengineering Conference, New York, NY, March 26-28, 2010.

Damcott M, Blochlinger S, Mantilla B, Foulds R, "Do Standing Programs Make a Difference?" Proceedings of the 2011 International Seating Symposium, Nashville, TN, March 3-5, 2011.

Damcott M, Blochlinger S, Mantilla B, Foulds R, "To Stand or Not to Stand?" Proceedings of the 2010 American Physical Therapy Association of New Jersey Annual Meeting, April 2010.

Damcott M, Blochlinger S, Mantilla B, Foulds R, “Dynamic vs. Passive Standing: Investigating the Impact on Bone Mineral Density.” Proceedings of the 2010 International Seating Symposium, Vancouver, Canada, March 5-8, 2010.

Damcott M, Blochlinger S, Mantilla B, Foulds R, "Impact of Dynamic and Passive Standing and Non-weight Bearing on the Bone Mineral Density in Immobilized Children." Proceedings of the 2009 European Seating Symposium Incorporating Assistive Technology, Dublin, Ireland, September 14-17, 2009.

Damcott M, Blochlinger S, "Overcoming the Fear: Transforming Dynamic Standing from a Clinical Idea to a Research Reality." 2009 Power of You Permobil Conference, Nashville, TN, July 8-10, 2009 and 2009 Lakeview Exposition, Edison, NJ, November 5-6, 2009.

Damcott M, Blochlinger S, Mantilla B, Foulds R, “Use of a Dynamic Stander to Increase Bone Mineral Density in Immobilized Children: A Pilot Study.” Proceedings of the Rehabilitation Engineering and Assistive Technology Society of North America 2009 Annual Conference, New Orleans, LA, June 23-27, 2009.

Damcott M, Blochlinger S, Mantilla B, Foulds R, “Increasing Bone Mineral Density in Immobilized Children Using a Dynamic Stander: Pilot Study.” Proceedings of the 35th Annual Northeast Bioengineering Conference, Harvard University, April 3-5, 2009.

Damcott M, Blochlinger S, Mantilla B, Foulds R, “Design of Dynamic Stander for Immobilized Children to Increase Bone Mineral Density.” Proceedings of the Rehabilitation Engineering and Assistive Technology Society of North America 2008 Annual Conference, Washington DC, June 26-30, 2008.

Damcott M, Blochlinger S, Mantilla B, Foulds R “Dynamic Stander Design for Immobilized Children to Increase Bone Mineral Density.” Proceedings of the 34th Annual Northeast Bioengineering Conference, Brown University, April 4-6, 2008.

To Ian and Izraelle.
Your love and support brighten every day
and I am so blessed to be able to share this
accomplishment with you.

To my mother, father, brother and sister.
Without your continued love and support,
I could never have accomplished all I have.

I also dedicate my dissertation to all the children with
orthopedic disabilities. Their love, innocence and hearts are the
continued motivating factors in my work every day.

ACKNOWLEDGMENT

I would like to thank Dr. Richard Foulds, my dissertation advisor, and Dr. Bryan Pfister, Dr. William VanBuskirk, Dr. J. Christopher Fritton and Dr. Sheldon Lin, committee members, for your vast knowledge and invaluable guidance. I could not have asked for a more appropriate and fantastic topic and I greatly appreciate the opportunity provided. A large thank you goes to Sheila Blochlinger as well, for her daily hard work, unlimited encouragement and immense dedication. The clinical knowledge and assistance and the friendship you provided allowed me to successfully complete the study and maintain my sanity. Thank you to the National Institute on Disabilities and Rehabilitation Research (NIDRR) for their funding through the Rehabilitation Engineering Research Center, Grant H133E0511-06. I also owe a debt of gratitude to my fellow lab members at New Jersey Institute of Technology, (Dr. Sergei Adamovich, John Hoinowski, Camila de Oliveira, Amy Boos, Olga Hizkiyahu, John Weimer, Katharine Swift, Amanda Irving, Brooke Odle, Diego Ramirez, Qinyin Qiu, Darnell Simon and Atul Narkhede), the teachers, aides and therapists at First Children's in Fanwood, NJ and Passaic County Elks Cerebral Palsy Center in Clifton, NJ and staff at Children's Specialized Hospital and my beautiful subjects and their families for their time, commitment and enthusiasm. Lastly, I owe my family an immense thank you. I thank Ian and Izraelle Mitchell for your love, understanding and patience. You are the sunshine to my every day, a great inspiration and the loves of my life. I thank Inta, David, Daryl and Erica Damcott for all your love and support as well. I owe you all more than words could ever say. I love you all and appreciate everything you have done to help guide me to where I am today.

TABLE OF CONTENTS

Chapter	Page
1 INTRODUCTION……..……..……..….	1
1.1 Background …….…….....	2
1.1.1 Bone Anatomy and Physiology ……....……...	2
1.1.2 The Bone Mechanostat ……...…….……...……....	6
1.1.3 Ambulation and Physical Exercise …..……..…….….....	8
1.1.4 Osteoporosis and Low Loading Environments …….……..	9
1.1.5 Passive and Dynamic Standing …….	10
1.1.6 Low-magnitude, High-frequency Vibration …….	11
1.1.7 Dual-energy X-ray Absorptiometery ……	13
1.2 Purpose and Hypothesis ……..…….….....	15
2 LONGITUDINAL STUDY ……. …….	17
2.1 Introduction …….....……...……..……..…….……....	17
2.2 Subject Population ……...…….……..……	17
2.3 Experimental Design ……...…….……..……	19
2.3.1 Equipment ..……...…….	19
2.3.2 Experimental Procedure and Data Collection …….…..	24
3 ANALYSIS OF DUAL-ENERGY X-RAY ABSORPTIOMETRY ...……..	28
3.1 Introduction …….…….……..……	28
3.2 Technology Behind Dual-energy X-ray Absorptiometery ....……..……	29
3.2.1 Attenuation and the R Value …..……...…….……..……	29

TABLE OF CONTENTS
(Continued)

Chapter **Page**

3.2.2 Calculation of Bone Mineral Density in Dual-energy X-ray Absorptiometry ….....…….……..…….. 31

3.3 Precision Analysis ……..……. 33

3.3.1 Impact of Angle of Femur Relative to the Axis of the Scan …….. 34

3.3.2 Impact of Rotation of the Knee …….. 35

3.3.3 Accuracy of the Edge Detection Algorithms During Image Analysis ….. 37

3.3.4 Determination of Tissue During Image Analysis …..……..…….. 43

3.4 Regions of Interest …….……. 46

4 ANALYSIS AND RESULTS ……...……. 52

4.1 Introduction ……..……..……..……... 52

4.2 Statistical Analysis ……..……..... 54

4.2.1 Statistical Analysis of Full Fifteen Months (Phase 1 through Phase 3)… 54

4.2.2 Statistical Analysis of First Six Months (Phase 1) ……... 54

4.3 Results for Full Fifteen Month Study (Phase 1 through Phase 3) ……..…….. 55

4.3.1 Analysis of the Three Regions of Interest …… 55

4.3.2 Analysis of the One Centimeter Regions of Interest …… 64

4.4 Results for First Six Months ……... 71

5 DISCUSSION AND CONCLUSIONS ……...…… 72

5.1 Discussion …..……..……..…… 72

5.2 Conclusions …….……...…..……..… 82

TABLE OF CONTENTS
(Continued)

Chapter **Page**

5.3 Future Work and Considerations ……..……..… 84

APPENDIX A: MATLAB SOURCE CODE FOR CONTROLLING THE DYNAMIC STANDER AND COLLECTING FORCES WITH LOAD CELLS … 86

APPENDIX B: MODIFIED PEARSON AND ROBINSON EDGE DETECTION ALGORITHM …… 93

REFERENCES …….. 96

LIST OF TABLES

Table		Page
2.1	Subject Population at the Start of the Study …….	19
2.2	Summary of Key Factors for Intervention Groups ...……...…….…….	26
3.1	Bone Mineral Densities (g/cm^2) of One Subject, Same Day, Same Leg ……..	44
4.1	Pooled Bone Mineral Densities for One Representative Subject ……..…	45
4.2	Mean Percent Changes in Bone Mineral Density for Henderson et al. ROIs …..	55
4.3	P-values for Bone Mineral Density in Henderson et al. ROIs ……...	58
4.4	Mean Percent Changes in Bone Mineral Content for Henderson et al. ROIs …..	59
4.5	P-values for Bone Mineral Content in Henderson et al. ROIs ……...	61
4.6	Mean Percent Changes in Region of Interest Area for Henderson et al. ROIs	61
4.7	P-values for Region of Interest Area in Henderson et al. ROIs …….....	63
4.8	Mean Percent Changes in Bone Mineral Density for One Centimeter ROIs …..	64
4.9	P-values for Bone Mineral Density in One Centimeter ROIs ……...	66
4.10	Mean Percent Changes in Bone Mineral Content for One Centimeter ROIs …..	67
4.11	Mean Percent Changes in Region of Interest Area for One Centimeter ROIs	67
4.12	P-values for Bone Mineral Content in One Centimeter ROIs ……...	70
4.13	P-values for Region of Interest Area in One Centimeter ROIs ……..…....	70
4.14	P-values for Bone Mineral Density for the First Six Months …….……...	71

LIST OF FIGURES

Figure		Page
1.1	Anatomy of the long bone ……	4
1.2	Anatomical structure of the long bone ……	5
1.3	Distal femur fractures ……	14
1.4	Lateral distal femur scanning method and regions of interest ……	15
2.1	Prone and supine passive standers ……	20
2.2	Dynamic standers ……	21
2.3	Dynamic stander footplate ……	22
2.4	Graphical User Interface (GUI) ……	23
2.5	General Electric Pediatric Lunar Prodigy Advanced™ ……	24
2.6	Lateral distal femoral scanning method ……	27
3.1	DXA two-component soft tissue model ……	31
3.2	Angle of femur from axis of scan ……	34
3.3	Original edges detected in pediatric and adult femur ……	38
3.4	Examples of edge detection using predefined edge detection algorithms from the MATLAB® image processing toolbox ……	40
3.5	5 x 5 logical valley detector ……	41
3.6	Example of bone edge detection results ……	42
3.7	Results of manually editing the enCORE point typing ……	45
3.8	Three Henderson et al. regions of interest for three subjects ……	47
3.9	Pooled bone mineral densities for one representative subject (3 ROIs) ……	48

LIST OF FIGURES
(Continued)

Figure		Page
3.10	Pooled bone mineral densities for one representative subject (one cm ROIs)	50
3.11	Eight one centimeter regions of interest ……	51
4.1	Percent changes in bone mineral densities for one representative subject	53
4.2	Mean percent change in bone mineral density (3 ROIs): dynamic standing	56
4.3	Mean percent change in bone mineral density (3 ROIs): passive standing	57
4.4	Mean percent change in bone mineral content (3 ROIs): dynamic standing	59
4.5	Mean percent change in bone mineral content (3 ROIs): passive standing	60
4.6	Mean percent change in area (3 ROIs):: dynamic standing	62
4.7	Mean percent change in area (3 ROIs):: passive standing	62
4.8	Mean percent change in bone mineral density (1 cm ROI): dynamic standing ….	65
4.9	Mean percent change in bone mineral density (1 cm ROI): passive standing …..	65
4.10	Mean percent change in bone mineral content (1 cm ROI): dynamic standing ….	68
4.11	Mean percent change in bone mineral content (1 cm ROI): passive standing …..	68
4.12	Mean percent change in area (1 cm ROI): dynamic standing ….....	69
4.13	Mean percent change in area (1 cm ROI): passive standing	69
5.1	Pooled bone mineral densities for one representative subject (one cm ROIs)	79
5.2	Pooled bone mineral densities for one representative subject (3 ROIs) ……...	79

LIST OF SYMBOLS

BMD	Bone Mineral Density
BMC	Bone Mineral Content
CP	Cerebral Palsy
WBV	Whole Body Vibration
DXA	Dual Energy X-ray Absorptiometry
CSH	Children's Specialized Hospital
NJ	New Jersey
GUI	Graphical User Interface
ROI	Region of Interest
IRB	Institutional Review Board
NJIT	New Jersey Institute of Technology
NDA	Non-disclosure agreement
ANOVA	Analysis of Variance

CHAPTER 1

INTRODUCTION

In 1892, surgeon Julius Wolff pioneered the study of bone physiology with the postulation that bone architecture adapts to its loading environment. Specifically, he observed that trabecular bone deposition tends to correspond to the orientation of the principle stresses applied on the bone. This postulation has been coined "Wolff's Law" and has evolved from a 'law' to a 'black box' in bone physiology which encompasses adaptations of bone morphology to mechanical stimuli (Pearson and Lieberman, 2004).

Harold Frost's (2003, 2004) "bone mechanostat" has begun to explain the underlying mechanisms enclosed in the 'black box' postulated by Wolff. Frost has unlocked the "biological 'machinery'" responsible for whole-bone strength in load-bearing bones and his work has led to clinical interventions in populations with low bone density and increased risk of fractures. Non-ambulant children have been determined to be one of such populations with low bone mineral density (BMD) and increased risk of non-traumatic fractures throughout their lifetime. In an effort to promote greater bone strength and decrease the number of fractures, the current therapeutic intervention in these children includes a passive standing program. In this program, the body is fully supported and continuous, stationary loading is applied to the long bones for a period of time each day. While significant literature discusses the potential clinical benefits of passive standing, current evidence does not show a consistent improvement in bone health.

Frost's bone mechanostat emphasizes the impact mechanical loading thresholds have on whole-bone strength. Two major mechanisms determine whole-bone strength; bone modeling and bone remodeling. Threshold levels relating to the magnitude of stresses and strains sensed by cells in the long bones of the body are responsible for determining which mechanism dominates. Studies investigating levels of physical activity in children have supported Frost's mechanostat, determining that the high-impact loading experienced during activities such as running, soccer, swimming and weight-lifting further improve BMD over daily activities such as walking and standing (Bailey 1999). In light of this, it appears that the passive clinical intervention could be improved with the addition of modest amplitude, cyclic mechanical loading. This study hypothesizes that incorporating a novel dynamic stander, which applies forces mimicking the natural walking gait, into the clinical standing protocols of non-ambulant children will increase known correlates of bone strength such as bone mineral content, cross-sectional area and bone mineral density, at a greater rate than the current passive standing protocols.

1.1 Background

1.1.1 Bone Anatomy and Physiology

The human skeletal system is a highly integrated and complex system comprised of a total of 206 bones which serve five main functions (Pearson and Lieberman, 2004):

1. **Support:** The skeletal system creates a framework for the human body and soft tissue, while providing an anchoring point for skeletal muscles.
2. **Protection:** Protection is provided for internal organs and soft tissues by the skeletal system.

3. **Movement:** The human skeletal system provides linkages to assist in movement at the sites of muscle attachments.
4. **Haematopoiesis:** Bones comprising the human skeletal system are the major source of red and yellow bone marrow. Red bone marrow produces red and white blood cells and platelets. Yellow bone marrow is responsible for storing lipids which serve as a chemical storage of energy for the body.
5. **Metabolism:** Bone is a reservoir of calcium, phosphorous and other essential minerals which can be released into the blood as necessary to maintain a homeostatic environment within the human body.

The classification of the bones in the human skeletal system includes five types (Martin et al. 1998):

1. **Long bones:** Including bones of the arm, leg, hand and foot which are characterized by a shaft and are greater in length than width.
2. **Short bones:** Characterized by their cube-like shape, short bones are composed primarily of trabecular bone and include the bones of the wrist and ankle.
3. **Flat bones:** Thin, curved bones in which two parallel layers of cortical bone surround trabecular bone. Examples include the ribs, shoulder blades, hip and cranium.
4. **Irregular bones:** Bones which do not fit any of the aforementioned categories are classified as irregular bones (i.e., vertebrae and facial).
5. **Sesamoid bones:** Bones imbedded in tendons are classified as sesamoid, which includes the patella of the knee.

Long bones are the primary load-bearing bones in the human skeletal system and thus the focus of this study (specifically the femur in the proximal leg). Therefore, the remainder of this section will spotlight the anatomical structure of long bones.

Long bones are comprised of three primary sections: the diaphysis, metaphysis and epiphysis (Figure 1.1). The diaphysis is the shaft of the bone. The metaphysis is the section responsible for the longitudinal growth of long bones, as it the region between the diaphysis and epiphysis where the growth plate is located. The epiphyses are the

proximal and distal ends of the long bones. The hollow space within the diaphysis of the bone is known as the medullary canal and is the location of the yellow bone marrow. The endosteum lines the medullary canal and contains osteoprogenitor cells. The outer sheathing of the long bone is known as the periosteum and contains blood vessels, nerves and lymphatic vessels. It also serves as the attachment point for ligaments and tendons.

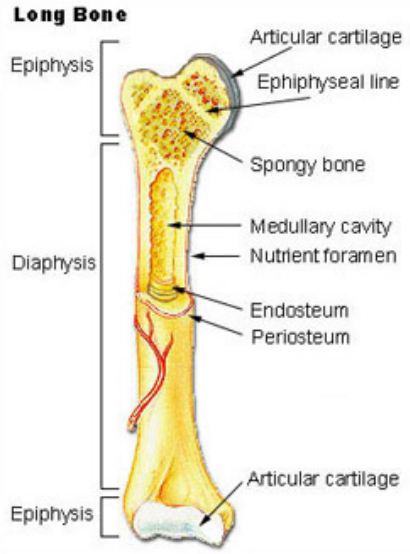

Figure 1.1 Anatomy of the long bone. Long bones consist of three primary sections: the diaphysis, metaphysis (not shown, but located between the diaphysis and ephiphyses), and the epiphysis.
Source: National Cancer Institute, http://training.seer.cancer.gov/anatomy/skeletal/classification.html.

The diaphysis is comprised of primarily cortical bone and the epiphysis is primarily comprised of trabecular bone. Cortical bone (also known as compact bone) and trabecular bone (also known as spongy or cancellous bone) are the two types of bone tissue. The major distinguishing factor of these two types of bone is their density. Cortical bone is a dense, tightly packed organization of bone tissue comprising approximately 80% of the skeletal system and located at the cortex of long bone. Trabecular bone is a porous bone located at the distal and proximal ends of long bones

(Martin et al. 1998). The mechanical properties of the bone tissues vary substantially due to the tissue's structure and composition (Pearson and Lieberman, 2004).

The tensile and compressive strength of bone is reinforced through its mechanical structure. The major constituent influencing the mechanical structure of bone tissue is collagen. Collagen fibers account for greater than 25% of the weight of bone tissue and are responsible for creating the framework on which bone is laid in an organized lattice. Type I collagen is organized into longitudinal bundles, known as osteons (Figure 1.2), which provide bone with a magnitude of elasticity and capitalize on the tensile strength of bone. A calcium-phosphorous mineral, known as hydroxyapatite, comprises approximately 65% of the weight of bone and is deposited within the gaps of the collagen to provide a magnitude of stiffness and compressive strength (Martin et al. 1998, Pearson and Lieberman, 2004).

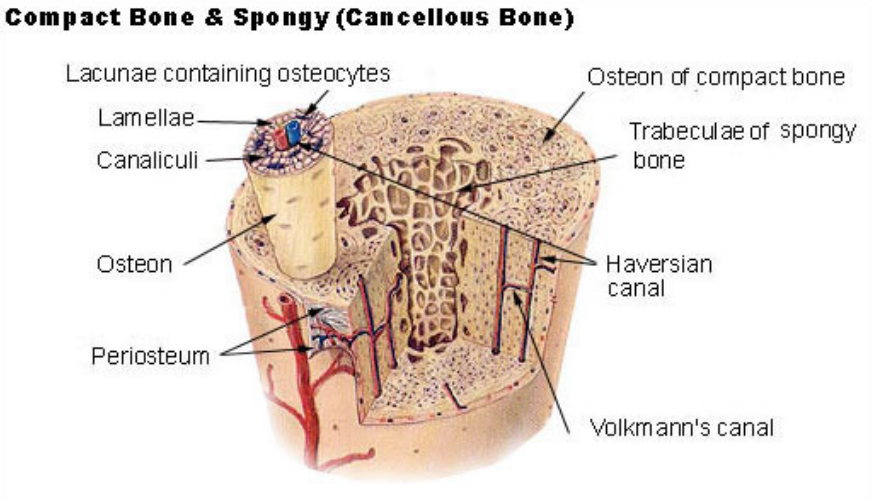

Figure 1.2 Anatomical structure of the long bone.
Source: National Cancer Institute, 2011. http://training.seer.cancer.gov/anatomy/skeletal/tissue.html.

Bone tissue is synthesized by the deposition of the collagen matrix directed by osteoblasts, bone cells responsible for bone formation. Once the initial collagen matrix is in place, osteoblasts then initialize mineralization of the collagen, the collagen orients to

provide maximal tensile strength and hydroxyapatite is deposited. Osteoblasts continue to deposit additional collagen matrix, trapping the previously set collagen matrix and osteoblasts. The osteoblasts entombed in the previous layer mature into osteocytes. Osteocytes are believed to play an intricate role in mechanotransduction; a bone's ability to sense loading, translate the signal and initiate response from other cells. Canaliculi (long processes) radiating from the cell body of the osteocyte are able to communicate bidirectionally with neighboring osteocytes, creating a complex connected network able to sense and respond to mechanical loads. While osteoblasts and osteocytes are responsible for synthesizing bone tissue, osteoclasts are responsible for resorbing existing bone (Pearson and Lieberman, 2004).

1.1.2 The Bone Mechanostat

Whole-bone strength is controlled through two primary processes: bone modeling and bone remodeling. These mechanisms are integrally controlled by the mechanical loads placed on a bone and are the mechanisms involved in Frost's bone mechanostat. While osteoblasts and osteoclasts are intricately involved in both processes, the mechanisms involved in modeling and remodeling are completely independent.

In bone modeling, osteoblasts and osteoclasts work independently, allowing bone resorption and formation to occur on different surfaces and large changes in bone structure and shape to occur. Bone modeling occurs primarily in children who are growing rapidly, in fracture healing and in bones in which the mechanical environment changes drastically for a sustained period of time. In long bones, bone modeling has the ability to increase the strength of bone by increasing the bone mineral content (density),

overall diameter (appositional growth) of the bone, the cortical shell thickness of the diaphysis or a combination of these three (Martin et al. 1998).

Whereas osteoblasts and osteoclasts work independently in modeling, in bone remodeling their actions are coupled and bone formation and resorption occur at the same location on the surface of the bone. Therefore, remodeling produces gradual changes in bone structure compared to the drastic changes associated with modeling. In a homeostatic environment, remodeling is responsible for continuously replacing old bone with new, without compromising the existing bone strength. However, as human beings age or in the absence of mechanical loading, bone formation begins to lag behind bone resorption, leading to a gradual decrease in bone strength (Martin et al. 1998).

Frost's bone mechanostat addresses the control of modeling and remodeling in response to the mechanical loads applied to the long bone. In utero, gene expression creates an individual's baseline bone strength. After birth, predetermined genetic thresholds control the modeling and remodeling mechanisms. These thresholds can be altered by different disease states or sustained changes to the bone's loading environment. If the mechanical loading creates stresses and strains that exceed the modeling threshold range, modeling is turned on to strengthen the bone. On the reverse side, if the stresses and strains remain below the lower threshold, then remodeling occurs to reduce the bone strength. For this reason, "no known bone-active humoral agents can replace mechanical loading effects in time and space on a bone's 'functional adaptations' to changes in its mechanical usage" (Frost 2004).

1.1.3 Ambulation and Physical Exercise

Studies investigating the impact of ambulation and physical exercise on BMD support Frost's claim that the mechanical loading environment is a critical component of bone health. Bailey et al. (1999) conducted a six-year longitudinal study in which the impact of physical activity on bone mineral accrual was investigated. Data were collected for 53 girls and 60 boys between 8 and 14 years of age with physical activity level classified as inactive, average (low-impact activities such as walking and standing) or active (high-impact activities associated with running and jumping). As BMD is dependent upon the area of the bone and therefore can be impacted by growth, bone mineral content (BMC) for the total body, lumbar spine and femoral neck were measured at 6 month intervals. Anthropometric data were collected to account for growth of the children. A 9% increase in total body BMC was found between active and inactive girls, with a 17% increase in boys.

Chad et al. (1999) conducted an 8-month study on the impact of physical activity with 18 children with cerebral palsy (CP). They found that children participating in a physical activity program two to three times a week for eight months experienced a 9.6% increase in femoral neck BMC, a 5.6% increase in volumetric BMD and an 11.6% increase in total proximal femur BMC. In the control group, a 5.8% decrease was observed in the femoral neck BMC, a 6.3% decrease in vBMD and a 3.5% increase in total proximal femur BMC. Each group consisted of a combination of non-ambulators, independent ambulators and ambulators with assistance. The effect between the children participating in the physical activity program and the control group was independent of ambulation status.

1.1.4 Osteoporosis and Low Loading Environments

The potential of mechanical loading to stimulate modeling and increase whole-bone strength has led to the investigation of numerous clinical interventions in individuals at increased risk of osteoporosis and bone fractures. Osteoporosis is defined as "a disease characterized by low bone mass and deterioration of bone structure that causes bone fragility and increased risk of fracture" (Surgeon General, 2004). The most prevalent form of osteoporosis is "primary" osteoporosis or osteoporosis that develops due to aging. Individuals, such as the children considered in this study, who become osteoporotic as a secondary condition of another condition or use of certain medications are said to have "secondary" osteoporosis. These individuals "typically experience greater levels of bone loss than would be expected for a normal individual of the same age, gender and race" (Surgeon General, 2004). One such developmental disability that often is associated with secondary osteoporosis is CP. In children and adolescents with CP, optimal peak bone mass is not achieved and therefore, up to 20% of non-ambulant children with CP will sustain a femoral fracture within their lifetime (Ko et al. 2006).

Non-ambulation in children with CP is one of the major aspects believed to be associated with secondary osteoporosis. Whether ambulant or non-ambulant, bones constantly have forces being applied to them associated with the Earth's gravitational pull and the forces applied by muscle flexions. The long bones of the body are inherently designed for periods of loading in which gravitational forces would be applied parallel to the axis of the diaphysis. This loading is significant as the forces applied perpendicular to the axis of the diaphysis (such as when an individual is lying supine) are 17% the magnitude of those applied parallel to the axis when the individual is upright. Studies

investigating the significance that forces in the upright position have on loading environments and bone strength have determined that individuals who experience long periods of bed rest or immobilization experience bone loss at a rate of 0.5 to 1.0% per month. When considering astronauts in low gravity environments, the bone loss is even more pronounced at 1.6% bone loss per month (Heer 2007). To slow the progression of the bone loss, interventions which apply a degree of mechanical loading in the upright, loaded position have been studied and implemented in populations at increased risk of osteoporosis.

1.1.5 Passive and Dynamic Standing

At the present time, one of the most common clinical interventions to apply mechanical loading to non-ambulant populations is passive standing. In passive standing, the individual is placed in the upright, loaded position with the body fully supported and continuous, stationary loading applied to the long bones. BMD outcomes in studies associated with passive standing have mixed results.

In a study by Caulton et al. (2004), the impact of the duration of a passive standing program on BMD in 26 pre-pubescent, non-ambulant children with CP was investigated. They concluded that a 60% mean increase in standing duration increased vertebral BMD, but had no significant impact on proximal tibia BMD. Therefore, increasing the standing duration is unlikely to produce a reduction in the occurrence of fractures in the long bones.

The design of the dynamic stander utilized in this study is a novel design; however the clinical intervention of dynamic standing is not a novel idea. Previous studies have investigated standers which provide varying degrees of ‘dynamic’ loading.

Gudjonsdottir and Mercer (2002a, 2002b) designed a dynamic stander which provided intermittent loading. Four children with CP participated in the study, with two in the dynamic stander and two in a conventional passive stander. Increases in BMD were observed in both children in the dynamic stander and one in the passive. Gudjonsdottir and Mercer concluded that the potential impact of dynamic standing on BMD warranted further investigation.

1.1.6 Low-magnitude, High-frequency Vibration

While significant progress has been made to understand the mechanism behind the impact of mechanical loading on whole-bone strength, questions on the direct biological response and therefore optimal parameters of the loading still remain. The dynamic stander (Gujonsdottir and Mercer 2002a) discussed in Section 1.1.5 provides a high magnitude, low frequency loading, which places large stresses on the skeleton to signal bone formation. While these forces are able to stimulate bone formation, Rubin suggests that the vibrations applied to long bones when the skeletal muscles attached to them are flexed during movement have a significant impact as well and the coupling of the two effects may hold the greatest promise (cited in Flinn, 2002). The impact muscles are believed to have on BMD has been simulated with the investigation of the impact of low-magnitude, high-frequency vibration.

Animal studies have demonstrated that low-magnitude, high-frequency vibration increases BMD in the distal femur, specifically in trabecular bone (Lanyon and Rubin, 1984, Rubin et al. 1995, 2001a, 2001b, 2002a, 2002b). Expanding the whole body vibration intervention to groups of individuals at increased risk of osteoporosis,

researchers have determined that low-magnitude, high-frequency vibration increases BMD in multiple areas of measurement.

An intention-to-treat study conducted on 70 postmenopausal women over a 12-month period demonstrated that low-magnitude, high-frequency vibration (30 Hz, 0.2g) has the potential to inhibit the progression of osteoporosis in the spine of lighter women (<65 kg). The women stood for 20 minutes a day and results concluded that compliance (>86%) had a significant impact on the success of the intervention (Rubin et al. 2004).

A 12-month trial conducted in young women with low BMD, observed that a minimum of 2 minutes/day of low-magnitude, high-frequency vibration (30 Hz, 0.3g) increased BMD in the lumbar spine and femoral midshaft, in both cortical and trabecular bone (Gilsanz et al. 2006).

A 6-month study in postmenopausal women who participated in a whole body vibration (WBV) (35-40 Hz, 2.28-5.09g), resistance training or no intervention concluded that 30 minutes of WBV increased the total hip BMD, while resistance training and no intervention produced no significant changes (Verschueren et al. 2004). Another similar study conducted in 2010, coupled the WBV with static and dynamic knee-extensor exercises and determined that BMD was increased in the hip, but no significant improvements were found in the lumbar spine or total body BMDs (Verschueren et al. 2010).

Ward et al. (2004) expanded WBV to ambulant children with disabling conditions and determined that BMD in the proximal tibia and spine increased with 6 months of treatment. However, while Ward et al. observed promising increases in ambulant children, a 9 month WBV study in non-ambulant children with CP yielded increases in

the vertebral BMD but no increases in proximal tibial BMD (Caulton et al. 2007). Thirty-one children with CP participated in a study in which they stood on a vibration platform (30 Hz, 0.3g) for 10 minutes/day for 6 months and stood without a vibration platform for an additional 6 months. The order of the vibration and standing were randomized among the children. Greater increases in the properties of the cortical bone of the tibia were observed during the vibration intervention, regardless of order (Wren et al. 2010).

1.1.7 Dual-energy X-ray Absorptiometry

One of the largest challenges researchers face when determining the impact of an intervention on bone health is to have an accurate and measurable outcome. As the overall clinical outcome of these studies is to increase the quality of life by decreasing the number of fractures an individual sustains, longitudinal studies investigating the occurrence of fractures over said individual's lifetime would be ideal. However, such studies would take decades to complete and therefore the number of lifetime fractures an individual sustains is not a practical outcome measure. Instead, most studies quantify bone health indirectly with measures of bone mineral density. Dual-energy x-ray absorptiometry (DXA) is the 'gold' standard bone densitometric technique used for children with orthopedic disabilities because of its fast scan time, precision, low dose of radiation, low cost and widespread availability relative to other imagining modalities such as computed tomography or magnetic resonance imaging (Gordon et al. 2008). The most significant limitation of DXA densitometry is its areal approximation of a volumetric measurement when calculating BMD (g/cm^2). Due to the areal nature of the BMD measurements in DXA, positioning of the subject during scan acquisition and

assumptions made in the algorithms during data analysis are critical to the precision of the study.

As the most common site of non-traumatic fractures in children with orthopedic disabilities is the transitional region between cortical and trabecular bone in the distal femur (Figure 1.3), the distal femur is the skeletal site investigated in this study (Leet et al. 2009). The common positioning used to acquire scans of the distal femur is to lay subjects in the supine position on the bed of the scanner. However, contractures of the hips and knees prevent children with orthopedic disabilities from lying in the supine position with their femur flush with the surface of the bed of the scanner. This could introduce significant error in the calculation of the BMD and therefore the supine position is not appropriate for these children.

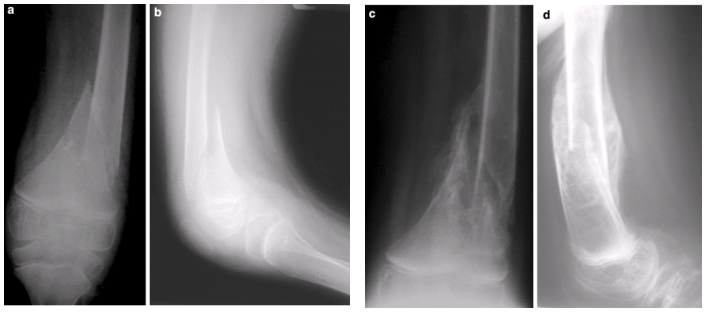

Figure 1.3 Distal femur fractures. The majority of non-traumatic fractures in pediatrics occur in the distal femur as seen the four images above.
Source: Leet et al. 2009.

While joint contractures prevent these children from lying in the supine position, their contractures do not prevent them from lying on their side. Therefore, the lateral distal femur scan is the accepted positioning for children with orthopedic disorders to determine the BMD of the distal femur in the regions of interest (ROIs) noted in Figure 1.4 (Harcke et al. 1998, Henderson et al. 2002).

Figure 1.4 Lateral distal femur scanning method and regions of interest. Left: lateral distal femur scanning position for children with cerebral palsy. Right: Regions of interest (ROIs) for later distal femoral scan in pediatric populations with disabilities.
Source: Harcke et al. 1998, Henderson et al. 2002.

The direct impact that assumptions made within the algorithms used to calculate the areal approximation of BMD have on the data collected in our study is discussed in depth in Chapter 3.

1.2 Purpose and Hypothesis

The purpose of this study was to investigate the impact of current conventional passive standing and a novel dynamic standing intervention which mimics the walking gait on the bone mineral density (BMD), bone mineral content (BMC) and bone diameter during a 15-month intervention in non-ambulant children. The principle hypothesis is that reciprocal loading applied during dynamic standing increases the BMD of the distal femur at a greater rate than the relatively static loading applied in passive standing.

Secondary investigations on bone health included the impact of each intervention on the underlying parameters of BMC and area (i.e. bone diameter) and the impact of each intervention on cortical and trabecular bone using the accepted regions of interest (ROIs) from current literature and novel one centimeter ROIs developed for this study.

Additional investigations into the implications of the positioning and software algorithms on the precision of the study and potential improvements were also conducted.

CHAPTER 2

LONGITUDINAL STUDY

2.1 Introduction

The objective of this study was to investigate the impact a dynamic standing protocol, which mimics walking, and a passive standing therapeutic protocol have on the BMD, BMC and ROI area in immobilized children. A fifteen-month study was completed with non-ambulant children standing in either a dynamic standing frame (designed, fabricated for this study, and described in sections below) or a passive standing frame currently available on the market. Outcome measures of BMD, BMC and ROI area were obtained with dual-energy x-ray absorptiometry (DXA).

2.2 Subject Population

As previous studies have determined an individual's peak bone mass is ascertained prior to puberty (Bass et al. 1998), subjects recruited for this study were pre-pubescent children between the ages of two and nine years of age. The subjects were recruited through Children's Specialized Hospital (CSH) in Mountainside, NJ and were required to attend either First Children School in Fanwood, NJ or Passaic County Elks CP Center in Clifton, NJ. All subjects had to be non-ambulatory and participating in a passive standing protocol prior to their inclusion in the study to ensure each had established a tolerance to standing. Subjects were excluded if they were receiving medications specifically prescribed for BMD or osteoporosis. However, due to the prevalence of seizures and use

of anti-convulsants in the population being considered in this study, subjects were not excluded if they were prescribed medication for seizures.

As described in the Experimental Procedure and Data Collection Section below, the fifteen month study was split into three phases: 0-6 months, 6-9 months and 9-15 months. Twenty subjects were originally identified for inclusion in the study. However four children were dropped prior to the commencement of Phase 1 of the study due to noncompliance issues in either signing consents, or acquiring the first DXA scan. An additional subject moved out of district prior to completion of the first six months of the study and another subject passed away. Therefore, fourteen subjects completed the first six month phase. Ten of the fourteen subjects were then continued for Phase 2 and 3 of the study. Four subjects were not continued from Phase 1 as one moved out of district, one was dropped due to logistical reasons and two subjects were unable to continue due to health concerns unassociated with the study. Table 2.1 below summarizes the demographics (gender, age and diagnosis), the standing intervention each subject was placed in, and the length of their participation in the study.

Table 2.1 Subject Population at the Start of the Study.

Subject	Gender	Age (Years)	Diagnosis	Standing Intervention	Length of Participation
1	F	7	CP	Dynamic	6 months
2	M	5	CP	Dynamic	15 months
3	F	5	CP/Stroke	Dynamic	15 months
4	F	7	CP	Dynamic	15 months
5	F	6	CP	Dynamic	15 months
6	F	6	CP	Dynamic	15 months
7	F	6	CP	Dynamic	15 months
8	F	4	CP	Dynamic	6 months
9	M	10	Seizures	Passive	6 months
10	M	4	CP	Passive	15 months
11	M	9	CP	Passive	15 months
12	F	4	CP	Passive	15 months
13	F	9	CP	Passive	6 months
14	M	9	CP	Passive	15 months

CP: Cerebral Palsy

2.3 Experimental Design

2.3.1 Equipment

Passive standers currently available on the market (Prospect Designs, Inc., Rifton, and EasyStand) were used throughout the duration of our study. Figure 2.1 illustrates an example of a Prospect Designs passive prone and supine stander used in the study.

Figure 2.1 Prone and supine passive standers. Left: Prone stander designed by Prospect Designs. Right: Supine stander designed by Prospect Designs.
Source: Prospect Design (2008).

As noted in the discussion of previous research, the concept of dynamic standing is not a novel idea. However, the dynamic standers which have been designed for previous research studies or are currently available on the market are not appropriate for the population of immobilized children with orthopedic disabilities considered in this study. Therefore, a novel dynamic stander which provides reciprocal forces mimicking the natural walking gait and includes consideration of the secondary health conditions of the population in its design was fabricated for this study. The stander was designed as a modified footplate which could be directly incorporated into current passive standers, thereby minimizing differences in transfer methods and therapeutic training protocols, while maintaining the integrity and stability of current standers.

Pneumatic actuators were incorporated with a hospital grade compressor to minimize the noise associated with the equipment and decrease the risk of initiating startle reflexes. In addition the system maintains the sterility and cleanliness of the

environment. Load cells were incorporated into the footplates in order to allow the forces being provided by the dynamic standing intervention to be recorded periodically throughout the study. Mechanical stops were placed on the distal end of the shafts to ensure that a maximum of one centimeter of vertical motion would not be exceeded, thereby decreasing the risk of joint contractures, hip dislocations and skin abrasions at the straps. Figure 2.2 below illustrates two dynamic standing prototypes used in the study. Figure 2.3 illustrates a close up of the dynamic system incorporated into a currently available passive stander. A full description of the design considerations, processes and fabrication can be found in Damcott, 2011.

Figure 2.2 Dynamic standers. Left: Supine dynamic stander. Right: Prone dynamic stander.

Figure 2.3 Dynamic stander footplate. The dynamic footplate was incorporated into the standing frame of current passive standers to minimize the training required to place and secure the children in the dynamic stander. Pneumatic actuators were used as they are relatively quiet and easily programmed in MATLAB®. Load cells were placed in between the top and middle plates to allow the forces being applied to the feet to be recorded throughout the study. Mechanical stops were placed on the distal end of the shafts to limit the vertical displacement to one centimeter and minimize the risk of chafing at the straps.

A custom program was written in MATLAB® 7.0. The program applies forces mimicking the walking gait according to the timing determined by Winter (1990), where T is equal to the total period for one gait cycle:

1. double stance for 10% of T (0-10% of T)
2. single stance (leg 1) and swing (leg 2) for 40% of T (10-50% of T)
3. double stance for 10% of T (50-60% of T)
4. swing (leg 1) and single stance (leg 2) for 40% of T (60-100% of T)

Pneumatic actuators were controlled by the program through the parallel port of the laptop. Force data were collected by the program periodically throughout the study through signal processes connected to the serial ports. A graphical user interface (GUI) was designed for users to easily input the desired session duration and the subject's weight. The interface included a start and emergency stop button for quick control of the dynamic stander and displayed the elapsed time of the session for the classroom staff. (Figure 2.4).

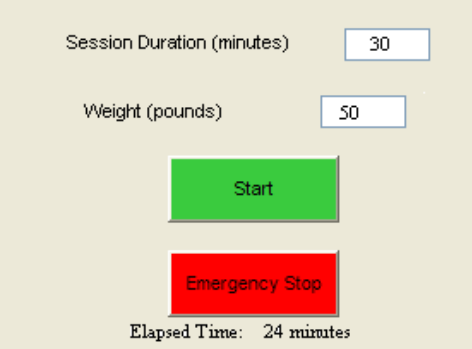

Figure 2.4 Graphical User Interface (GUI). The graphical user interface designed as the interface for the custom MATLAB® program. The interface allows the user to input the desired session duration and the weight of the subject. The start and emergency stop buttons control the dynamic stander and the elapsed time is displayed for the classroom staff.

The General Electric Pediatric Lunar Prodigy Advanced™ dual-energy x-ray absorptiometery densitometer (Figure 2.5) was used to acquire all scans. All scans were analyzed using the General Electric enCORE software version 9.30.044. The same research staff and technologist were present for all scans. The forearm scan modality of the Prodigy Advanced was used to acquire the scans as it is the only scan modality within the encore software that allows the necessary number of user-defined custom ROIs (explained further in Section 3.4). A successful Quality Assurance diagnostic test was

completed prior to each day of scan acquirement to ensure the densitometer was within the necessary calibration ranges. Based upon the subject height and weight entered by the technologist, the scanner computer determined which scanning mode would be used (thin, standard, thick). To determine in which mode the child should be categorized, the software compared the subject's height, weight and age to a normalized database. Each scan gave the BMD in g/cm^2, BMC in g and area in cm^2 for the selected regions of interest (ROIs). The ROIs used in this specific study are described in Chapter 3.

Figure 2.5 General Electric Pediatric Lunar Prodigy Advanced™. This densitometer was used to acquire all scans for the study. The same research staff and technologist were present for all scans. GE enCORE software, version 9.30.044 was used to analyze the scans.
Source: GE Lunar Corporation, Madison, WI, 2011).

2.3.2 Experimental Procedure and Data Collection

Institutional Review Board (IRB) approval was obtained through New Jersey Institute of Technology (NJIT), Newark, NJ. Subjects were screened to ensure they fit the inclusion and exclusion criteria listed in Section 2.2. The study protocol was described and a video demonstration of the dynamic stander was presented to the subjects and their families prior to obtaining their written consent/assent.

The study was split into three phases:

1. Month 0 to Month 6: Fourteen subjects participated in Phase 1 with eight standing dynamically for six months and six standing passively.
2. Month 6 to Month 9: Ten subjects were continued from the initial six months. All subjects stood in passive standers during the three months of Phase 2.
3. Month 9 to 15: After the three month period of passive standing, the ten subjects were returned to their previous research intervention with six returning to dynamic standing and four to passive.

All standing was completed in each subject's daily classroom. In order to provide minimal disruption, the therapeutic protocol already established by the schools was followed with each subject standing five days a week for 30 minutes per day. As illnesses, personal conflicts and school closings prevented 100% compliance, the total number of days and total minutes each subject stood throughout the study was tracked. Compliance within the passive standing group was 85% (range: 74%-99%). Compliance within the dynamic standing group was 83% (range 69%-95%). Three nutritional analyses were completed during Phase 1 of the study to confirm that no significant changes in diet occurred.

Originally, the subjects were to be randomly assigned to an intervention group. However, logistical considerations in staffing and equipment prevented this randomization. Therefore, all subjects at First Children participated in the dynamic standing intervention and all subjects at the Passaic County Elks CP Center participated in the passive standing intervention. Table 2.2 summarizes key factors for each intervention group.

Table 2.2 Summary of Key Factors for Intervention Groups

	Passive Standing Phase 1	**Dynamic Standing Phase 1**	**Passive Standing Phase 2**	**Dynamic Standing Phase 2**
Gender	4 male 2 female	1 male 7 females	3 male 1 female	1 male 5 female
Age (years)	Mean: 7.5 St. Dev.: 2.7	Mean: 5.75 St. Dev: 1.0	Mean: 6.5 St. Dev: 2.9	Mean: 5.8 St. Dev: 0.75

Dual-energy x-ray absoptiometry scans were obtained for each subject in three month intervals. All subjects received scans at 0-, 3-, and 6-months in Phase 1. Those subjects who were continued in Phase 2 and 3 also received scans at 9-, 12-, and 15-month intervals. The lateral distal femoral scanning method was employed to obtain the scans. Research staff for this study was trained in the lateral distal femoral scanning procedure prior to the commencement of the study by Ms. Heidi Kecskemthy (personal communication, February 21, 2011), a member of the team (Henderson et al 2002) which created the method and who has over ten years experience in the method and trained dozens of research teams. Each subject was laid in the lateral position as illustrated in Figure 2.6. Two scans of each leg were obtained at each appointment, with the subject's leg repositioned between the scans to verify the precision of the study during analysis. The 1/3 forearm scanning mode of the enCORE software was used to acquire all scans as it allows the freedom to set the necessary custom ROIs in later analysis.

Figure 2.6 Lateral distal femoral scanning method. Pictured above is the positioning for a right leg lateral distal femoral scan. The subject was laid in the lateral position with the right leg (leg of interest) against the bed of the DXA machine. The contralateral left leg was elevated and flexed to be positioned out of the viewing frame. Due to the degree of spasticity in many of the subjects, the femur of the leg of interest was placed as close to parallel to the axis of the scan as possible.

CHAPTER 3

ANALYSIS OF DUAL-ENERGY X-RAY ABSORPTIOMETRY SCANS

3.1 Introduction

Dual-energy x-ray absorptiometry (DXA) is the 'gold' standard for obtaining bone mineral densities in children with orthopaedic disabilities as it is relatively quick to scan the child and produces a low dose of radiation when compared to computed tomography or magnetic resonance imaging. However, one drawback to DXA is its estimation of a three-dimensional volumetric quantity as a two-dimensional areal measurement. It has been widely published that the areal nature of DXA to estimate the volumetric property of BMD causes the measurements to be "influenced by bone size, with larger bones having artificially inflated areal BMD measurements" (Specker and Schoenau, 2005) and the density of smaller bones often being underestimated. While the pediatric version of the General Electric Lunar Prodigy Advanced™ densitometer and enCORE software was used to obtain the scans in this study, the small stature, small bones and low BMD of the subjects proved to amplify the error in the same day/same leg scans. This chapter details the error found within the preliminary analysis of the data, the potential factors responsible for the error and the correction used for this study. Furthermore, suggestions for potential methods to correct sources of error in future studies are described.

3.2 Technology Behind Dual-energy X-ray Absorptiometry

3.2.1 Attenuation and the R Value

As the name suggests, DXA densitometers use a dual energy x-ray beam to calculate the BMD using the underlying physical concept that tissue composition will determine photon attenuation in vivo. Densitometers contain a photon source, filter and detector. The GE Lunar Prodigy Advanced photon source emits x-rays which consist of photon energy of 76 keV. A K-edge photon filter then filters the x-ray at two main photon peaks, about 40 keV and 70 keV. The photons are then passed through the subject and quantified with the use of a cadmium zinc telluride detector. Attenuated photons which fall within a pre-determined range are counted as belonging to one of the two photon beams.

As the photons pass through the subject, physical interactions occur with the tissues of the body that reduce the beam intensity. The photons are attenuated in vivo through scattering or absorption, specifically Compton scattering or photoelectric effect. The fractional decrease of the beam intensity due to attenuation is dependent upon the linear attenuation coefficient of the material it is passing through and the path length, as demonstrated by the classic attenuation formula:

$$I = I_0 e^{-\mu \times L} \tag{3.1}$$

where I_0 is the initial photon intensity, μ is the linear attenuation coefficient and L is the path length. While this significantly simplifies the physics behind the technology used in DXA calculations, it demonstrates the principle concept that the beam intensity quantified at the detector is dominantly impacted by the attenuation coefficients of the materials the beam transverses through. The initial photon intensity and path length of the beam remain constant throughout the viewing field. Therefore, the different intensities

sensed by the detector must be related to the attenuation coefficients of the materials the beam is passing through (Pietrobelli et al. 1996).

In equation 3.1, the linear attenuation coefficient is dependent upon density. As the human body is a heterogeneous mixture of tissues with different densities, the photon attenuation of a monoenergy beam can best be described by:

$$\ln(I/I_0) = \sum (-f_i \times \mu_{mi} \times M) \quad (3.2)$$

where I_0 is the initial photon intensity, f_i is the mass fraction of the *i*th component as heterogeneous absorber, μ_{mi} is the mass attenuation coefficient of the *i*th component and M is the mass per unit area (corresponding to the mass per pixel for DXA) (Pietrobelli et al. 1996).

Applying these principles to a dual-energy photon beam, a ratio (R) of the attenuation at the lower energy (L) to the attenuation at the higher energy (H) can be expressed by:

$$R = \sum [(-f_i \times \mu_{mi})_L] / \sum [(-f_i \times \mu_{mi})_H]. \quad (3.3)$$

The R values of various elements and components present in the human body have been quantified in previous studies. For instance, the R values for fatty acids and triglycerides are in the range of 1.21 and for water, intracellular fluid and extracellular fluid in the range of 1.35 – 1.38. The R value for minerals and bone however are twofold greater, in the range of 2.72 and 2.86, respectively (Pietrobelli et al. 1996).

In a system where a mixture of two components exists, the known mass coefficients for each component at both energies and the measured R values can be used to solve for the mass fraction of each component. This is the principle behind DXA calculations. The total R value of the system can be summarized as:

$$R = f_1 \times R_1 + f_2 \times R_2 \quad (3.4)$$

where

$$f_1 + f_2 = 1 \quad (3.5)$$

Rearranging the fractions and substituting, the mass fractions of each component can be expressed as (Pietrobelli et al. 1996):

$$f_1 = (R-R_2)/(R_1-R_2) \quad (3.6)$$

$$f_2 = (R_1-R)/(R_1-R_2) \quad (3.7)$$

3.2.2 Calculation of Bone Mineral Density in Dual-energy X-ray Absorptiometery

Equations 3.6 and 3.7 summarize how in a two-component system the mass fraction of each component can be calculated with the measurement of the R values. For the purposes of DXA, the constituents of the human body are categorized as fat, bone mineral and residual or "soft lean tissue" (Figure 3.1).

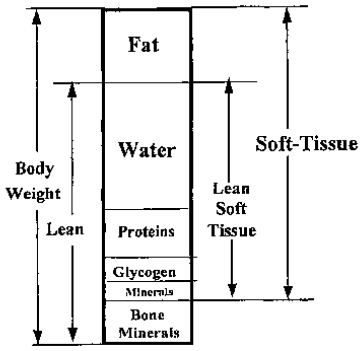

Figure 3.1 DXA two-component soft tissue model.
Source: Pietrobelli et al. 1996.

Although the constituents are categorized into three components, it would require three photon energies to separate the components. Therefore, in the estimation of the BMD, each separate pixel within the scan field is separated into pixels with soft tissue

only (fat + soft lean tissue) and soft tissue + bone mineral. The R value for every pixel is calculated. As mentioned previously, the R value of bone mineral is twofold that of soft tissue, so the pixels can be separated through 'point typing' by setting predetermined threshold levels for R values. The point typing algorithms then use histogram analysis, iteration and image processing techniques to determine whether the pixel contains bone mineral and where the skeletal boundaries are. Assumptions of minimal bone size and absence of "islands" of bone are incorporated into the imaging processing techniques. Assumptions of soft tissue in imaging algorithms include weighted soft tissue estimation in pixels which contain bone, as there is more skeletal muscle near the long bones and more adipose tissue near the skin (Pietrobelli et al. 1996).

Using the measured attenuation, the R values known for each component and the assumptions in the imaging processing techniques, the DXA software is then able to determine if the pixel is fat + soft lean tissue or soft tissue + bone mineral. Once the point typing has been determined, the bone mineral 'content' (g) in each region of interest (ROI) is calculated by subtracting the 'content' of the fat + soft lean tissue from the 'content' of the soft tissue + bone mineral. The area (cm^2) of bone within the ROI is calculated by determining the number of pixels enclosed by the edges of the bone (from the point typing) and the boundaries of the defined ROI and multiplying that by the known area of each pixel. The BMD (g/cm^2) of the ROI is then calculated by dividing the BMC by the area (Pietrobelli et al. 1996).

3.3 Precision Analysis

In bone densitometry, precision is a quantitative measure of "the ability to reproduce the same numerical result in the setting of no real biologic change when the test is repeatedly performed in an identical fashion" (Bonnick et al. 2001). As DXA measurement in children with orthopedic disabilities is known to have limitations in precision, an analysis of the precision in this study was completed on the same day/same leg scans of the lateral distal femur. A preliminary investigation of the data in this study revealed that the repeatability error of the measures in our study was twice the accepted level. Previous literature has established that the accepted error in the femur is 5% (Bloomfield et al. 1996, Gordon et al. 2008). The error for this study approached 10%. This revelation spurred an in-depth investigation into the source of the error in the scans.

Precision in bone densitometry is most greatly impacted by the positioning of the subject during scan acquisition and the data analysis. In subjects with low BMD, factors related to the algorithms can have a significant impact on the calculation of the BMD. With this consideration, four factors were determined to warrant further investigation into their impact on the precision of this study:

1. The angle of the femur relative to the axis of scan in the viewing frame.
2. The rotation of the knee during scan acquisition.
3. The accuracy of the bone edge detection algorithms during image analysis.
4. The determination of the tissue during image analysis.

The impact of each factor and the resolution of the problem are described in the following sections separately.

3.3.1 Impact of Angle of Femur Relative to the Axis of the Scan

A study investigating the precision of the GE Lunar Prodigy for pediatric whole body indicated that the whole body DXA results in pediatrics is highly reproducible. However, the same study noted that while whole body measurements are highly reproducible, DXA measures of bone density at specific skeletal sites had decreased reproducibility, quoting "even subtle differences in position between scans may change the results of the DXA algorithm for bone and soft tissue" (Marguiles et al. 2005). With this is mind, the positioning of our subject's femur during scan acquisition was the first factor investigated.

Ideally, in the lateral distal femoral DXA procedure, the femur is aligned parallel to the axis of the scan. However, when considering the population for this study, the prevalence of joint contractures and spasticity make it impractical to place the femur parallel to the axis of scan during every scan acquisition. The angle of the femur from the axis of scan within this study ranges from 0 to 17 degrees as demonstrated in Figure 3.2.

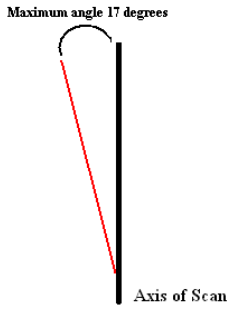

Figure 3.2 Angle of femur from axis of scan. The angle of the femur in relation to axis of scan ranged from parallel with the axis (0 degrees) to a maximum of 17 degrees.

After acquiring the scans, research staff on this study once again met with Ms. Kecskemthy (personal communication, February 21, 2011) to discuss the potential sources leading to the decreased precision of the lateral distal femoral method within the

GE Pediatric Lunar Prodigy Advanced™ system. During this meeting, the research staff was able to view scans from previous studies conducted by Ms. Kecskemthy. At his time, it was observed that in a number of images from previous studies she had worked on, the femur was not parallel to the axis of the scan, showing similar angles to those in this study. Discussions with Ms. Kecskemthy, surrounding the impact this had on the error in their studies, concluded that while it is not the ideal positioning, it is clinically acceptable and should not be a significant source of decreased precision.

3.3.2 Impact of Rotation of the Knee

The nature of DXA to estimate the volumetric measurement of BMD as an areal approximation leads to measurements which are "influenced by bone size with larger bones having artificially inflated BMD measurements" (Specker and Schoenau, 2005) and the BMD of smaller bones often being underestimated. Algorithms associated with DXA data analysis often simplify the calculations by incorporating the theoretical simplification that long bones can be modeled as perfect cylinders. In truth, bones are not perfect cylinders with a cross-sectional diameter that varies in relation to the angle at which the cross-section is being viewed. Therefore, the angle of rotation of the knee during positioning could have a significant impact on the diameter of the bone in the viewing field, thereby decreasing the precision of the area calculated by the enCORE software.

To investigate the impact of the rotation of the knee on the precision of the lateral distal femoral BMD measurements, a swine leg was scanned at various angles. A swine leg was procured from a local butcher with the knee joint and soft tissue of the lower limb intact. A steel pin was inserted into the femoral head and tibial head of the swine leg

to allow researchers to mark the positioning of leg within the viewing frame. The pin in the femoral head also allowed researchers to measure the angle of rotation of the leg. The swine leg was wrapped securely in plastic to ensure that the sterility of the hospital setting was maintained throughout the scanning session.

The swine leg was scanned on the GE Pediatric Lunar Prodigy Advanced™ densitometer at CSH. The swine leg was placed parallel to the axis of scan for each scan and care was taken to ensure no confounding factors in positioning were present. The degree of rotation of the knee was the only independent positioning variable present. Using the pin in the femoral head of the leg as a measurable landmark, the femur of the swine leg was rotated from 0 to 30 degrees at 5 degree intervals. A minimum of two scans were obtained at each incremental angle. The swine leg was then rotated to 90 degrees where two scans were obtained.

Four scans were obtained at 0 degrees. Preliminary analysis of these four scans demonstrated an anomaly not originally expected. The calculated precision between the first and second scans at 0 degrees was within the acceptable 5%. The precision between the third and fourth scans at 0 degrees was also within the acceptable 5%. However, when calculating the precision between the two sets, the precision decreased to the 10% range. As the positioning was strictly controlled during scan acquisition, it was apparent that there were other factors influencing the precision of the system. The densitometer had passed its QA prior to data acquisition, so focus into the source of decreased precision turned to the principles and assumptions behind the algorithms in the enCORE software. Upon further investigation of the four scans at 0 degrees, it was determined that the point typing (described in 3.2) between the scans in each group were similar, however

between the groups the point typing differed significantly. The point typing in the scans were corrected as described in the following two sections and the BMD, BMC, and area were recalculated. After the point type correction was performed, the precision of all four scans fell within the acceptable 5%.

With the precision of the four scans at 0 degrees within the acceptable precision range of 5%, the rest of the scans at each angle were analyzed. With minimal point typing corrections in the scans, the precision between the scans at each individual angle all fell within 5%. Further analysis of the BMD, BMC and ROI area of the scans between the angles of rotation verified that knee rotation between 0 and 20 degrees did not produce a significant decrease in the precision of the calculated BMD, BMC or ROI area measurements. As the maximum rotation of the knee clinically seen in this study was within the range of 0 to 20 degrees, it was concluded that the rotation of the knee during positioning was not a significant factor contributing to the decreased precision. However, the revelation of the impact of point typing on the precision during this investigation spurred exploration into the algorithms used in the calculation of the BMD, BMC and area in the following sections.

3.3.3 Accuracy of the Edge Detection Algorithms During Image Analysis

As discussed in Section 3.2, point typing algorithms in DXA rely heavily on preset threshold levels in their determination of the material in each pixel. These algorithms are known for their "inability to detect the bone edge in individuals with low bone density" (Fewtrell 2003). While the pediatric version of the enCORE software aids in more accurate determination of the bone edges by accounting for lower bone density and thus different threshold levels in the pediatric software relative to an adult population, the

children within this study are hypothesized to have low bone density for age matched children. Therefore, the threshold levels set for 'normal', healthy children may be inappropriate for the population in this study.

While viewing the images, the discrepancy in the placement of the bone edge by the software in relation to the actual bone edge on the image is apparent under visual inspection in the majority of the pediatric subjects enrolled in the study. However, Figure 3.3 demonstrates how the placement of the bone edges on the image of a lateral distal femur of a healthy adult using the same densitometer is more accurate.

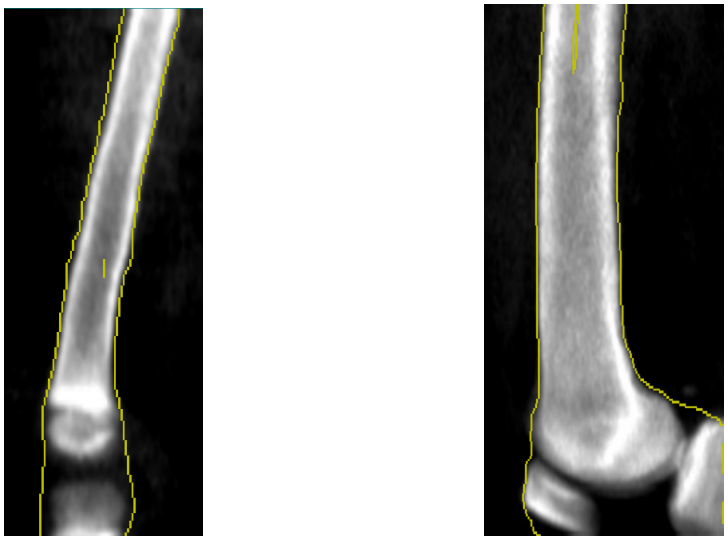

Figure 3.3 Original edges detected in pediatric and adult femur. The edges detected by the enCORE software are indicated by the yellow lines on the images. Left: Right distal femur of a pediatric subject. Right: Right distal femur of an adult subject. With the naked eye, it is apparent that the edge detection in the femur of the adult subject is more accurate than the pediatric bone edge detection. This discrepancy in edge detection algorithms is one drawback when using DXA. Also apparent are the islands within the bone that are not detected as bone.

The clinically acceptable solution to the limitations in the edge detection algorithms of DXA is currently to manually 'clean' the images. While enCORE does allow the technician to manually edit the bone point typing, thereby improving the edges and precision, this is not ideal. Manually editing the bone point typing is technician

dependent and thus limits multi-site studies and comparisons between studies. Therefore researchers in this study sought to investigate a more concrete method of correcting the edges.

The first parameter of the edge detection algorithms to investigate is the impact of the predefined threshold levels. As seen in Figure 3.3, island within the bone are incorrectly identified as tissue other than bone. As the bone surrounding these areas is correctly defined as bone, this suggests an error in the threshold levels of the algorithms. Due to the proprietary nature of the enCORE software, the specific threshold levels used to determine the bone edges could not be accessed. Therefore, I sought to investigate if the edge detection algorithms and threshold levels could be improved by exporting the .jpg images of the DXA scans to MATLAB® 7.0.

Once the .jpg images were imported into MATLAB®, predefined edge detection algorithms in the image processing toolbox were applied. The Sobel, Roberts and Canny edge detection algorithms were initially investigated. However, as seen is Figure 3.4, these edge detection algorithms were not appropriate for the detection of the bone edges in this application.

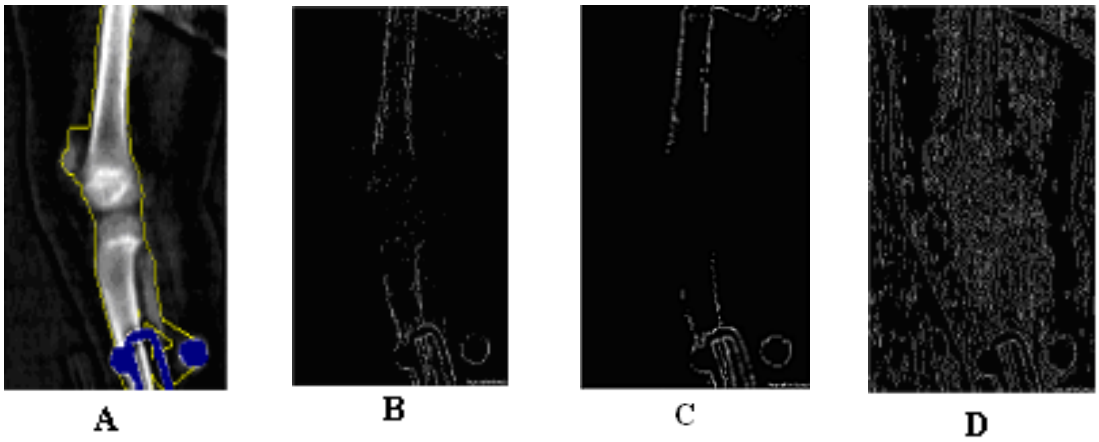

Figure 3.4 Examples of edge detection using predefined edge detection algorithms from the MATLAB® image processing toolbox. A) The original edges as defined by the enCORE software are displayed in yellow. B-D) Edge detection using MATLAB®'s predefined algorithms as follows: B) Sobel, C) Roberts and D) Canny.

As the predefined edge detection algorithms within the imaging processing toolbox were not appropriate for this study's application, a MATLAB® function was written to implement an edge detection algorithm postulated by Pearson and Robinson (1985). The Pearson and Robinson algorithm was written specifically for the edge detection of curved objects (such as the curves of the face to produce cartoon images or the edges of the finger in sign language.) The algorithm uses a luminance valley method to detect the edges of a curved surface in which the illumination of the edges is impacted by tangential reflections to the line of sight of the camera. As a common assumption in the edge detection of the femur is that it can be approximated as a cylindrical cross-section, an algorithm using luminance valleys to account for tangential reflections would be more appropriate than the previously investigated edge detection algorithms.

The Pearson and Robinson algorithm uses luminance valleys to detect whether a pixel constitutes an edge by using a 5 x 5 logical valley operator as shown in Figure 3.5. Each individual pixel is tested to determine if it constitutes a horizontal, vertical or diagonal valley. The ability to set individual thresholds for each direction provides the

Pearson and Robinson algorithm a robustness that was concluded to be appropriate for the application in this study. Figure 3.6 demonstrates the increased accuracy of the edge detection of bone associated with the algorithm. The full code for the novel MATLAB® function incorporating the modified Pearson and Robinson edge detection algorithm is included in Appendix B.

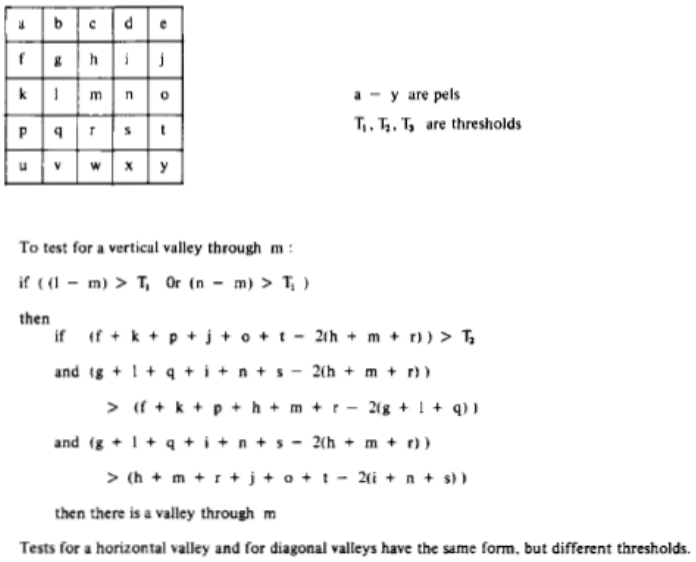

Figure 3.5 5 x 5 logical valley detector.
Source: Pearson and Robinson, 1985.

Bone Edges GE enCORE Software

Bone Edges Manually Adjusted

Bone Edges Found with Pearson Robinson Method

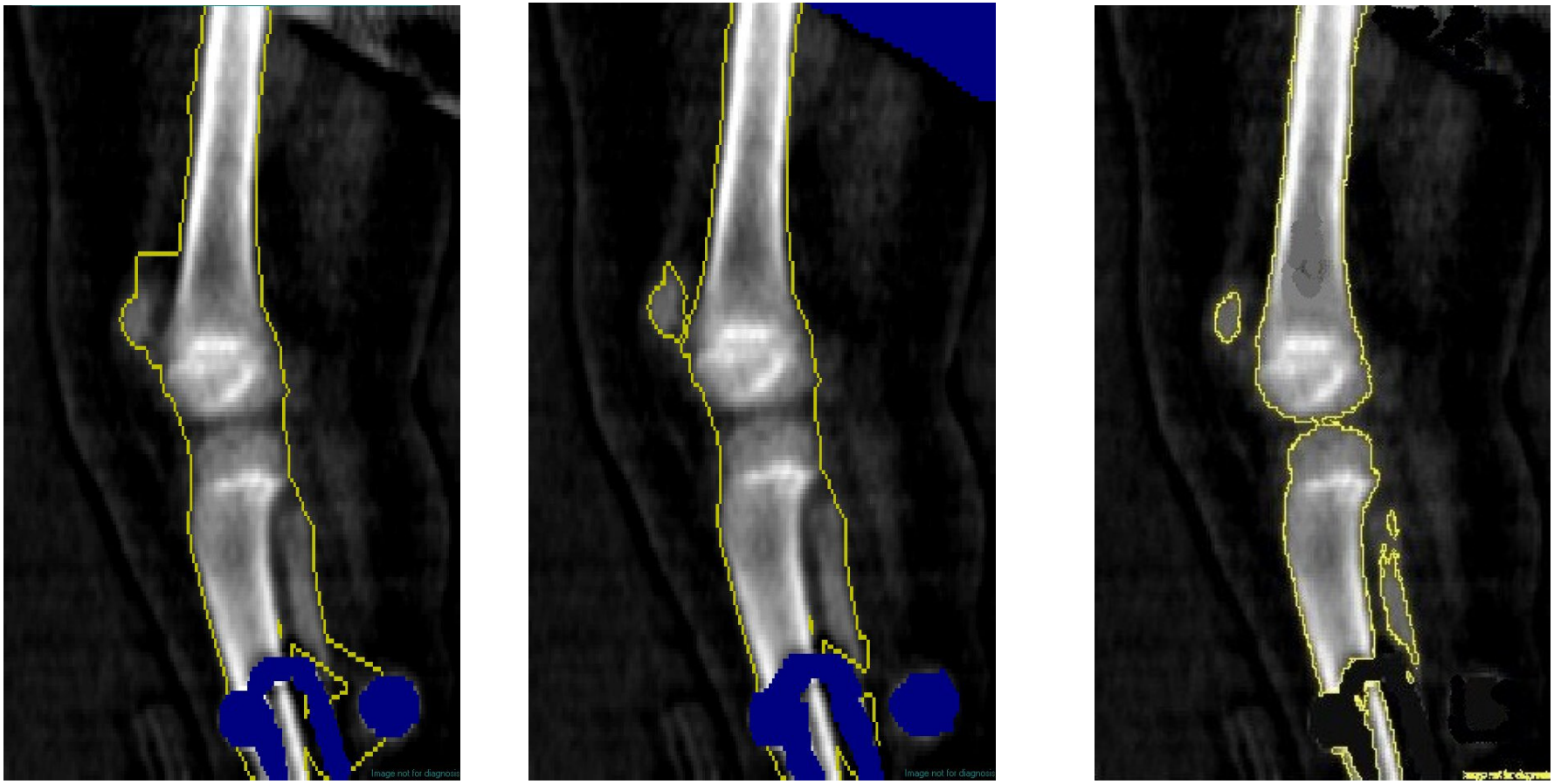

Figure 3.6 Examples of bone edge detection results. Using the unedited output of the GE encore software (extracted from radiological image data), the manual editing that is currently acceptable in research and clinical practice (based on the luminance image) and the edges extracted by custom software implementing a modified Pearson-Robinson luminance valley method (Pearson and Robinson, 1985) the edges were found in yellow. Accuracy of edge detection progresses from left to right, indicating that the use of the Pearson Robinson method would potentially enhance the accuracy of DXA scans in children with very low bone mineral content. The blue in the images signify 'artifact', which is omitted

With an appropriate edge detection algorithm identified, the next logical step would have been to import the new bone edges into the enCORE software to allow the BMD, BMC and area to be calculated. However, in order to import the new edges into enCORE, access to the proprietary system files is necessary. I pursued a tertiary non-disclosure agreement (NDA) between General Electric Healthcare, Children's Specialized Hospital and New Jersey Institute of Technology. At the time of publication of this document, the NDA had been acquired but access to the system files was still pending. Therefore, incorporation of the new edge detection algorithm will be included as a future research consideration and not used in the analysis of the data in this study. In light of the time constraints of the study, the clinically accepted method of manually editing the bone edges was utilized in data analysis for this study. All manual modification of the bone edges in this study has been completed by one individual, Ms. Damcott.

3.3.4 Determination of Tissue During Image Analysis

The reliance of point typing algorithms on threshold levels can greatly impact the accuracy of tissue classification as well. In the enCORE software, point typing is categorized into five broad categories: 'bone', 'tissue', 'neutral', 'air' and 'artifact'. 'Bone' incorporates bone, 'tissue' includes all soft and lean soft tissue (i.e., muscle, skin, tendons, and fat), 'neutral' is defined as a transitional border between two materials, 'air' refers to any material within the viewing frame that is located outside the body's boundaries and 'artifact' encompasses any objects which should not be in the viewing frame. When calculating the BMC of an ROI, the enCORE software assumes the ROI extends over the following order of material interfaces: 'tissue', 'neutral', 'bone',

'neutral' and 'tissue'. As this assumption is incorporated into the algorithms, if the expected interfaces are not present, the algorithms are not robust enough to overcome the inaccuracy in the point typing and the precision of the data analysis significantly decreases. In the majority of the scans analyzed in this study, no or limited tissue was detected or only tissue in the lower 1/3 of the viewing frame was detected, leading to the majority of the quadriceps and hamstring muscles not being detected as tissue. The inaccuracy of the tissue detection in the scans in which no or limited tissue was detected is attributed to inappropriate threshold levels within the algorithms for the significantly disabled subject population. However, as access to system files was not obtained in the time frame associated with this publication, an in-depth investigation into appropriate threshold levels for this population of children was not possible.

The inaccuracy of the tissue detection in only the lower 1/3 of the viewing frame is inherent to an assumption specifically applied in regard to using the 1/3 forearm scanning modality. Similar to the assumptions made in bone point typing that the skeleton consists of continuous bodies without "islands" and long bones are above a minimum size, the 1/3 forearm scanning mode assumes that the majority of the tissue in the forearm is located adjacent to the elbow joint. Therefore, the tissue in the lateral distal femoral scans is prematurely truncated (Figure 3.7) and the majority of the quadriceps and hamstring muscles are defined as 'neutral'. Without access to the system files of the enCORE software, the data analysis of this study must include this assumption in the analysis procedure.

As neither of the sources of inaccuracies in the tissue detection can be resolved without access to the system files, the clinically accepted method of manually editing the

not only the bone edges, but additionally the tissue detection will be utilized in data analysis for this study. All manual modification of the tissue point typing in this study has been completed by one individual, Ms. Damcott. Figure 3.7 and Table 3.1 illustrate that a precision within the 5% range can be achieved once the manual point typing has been completed.

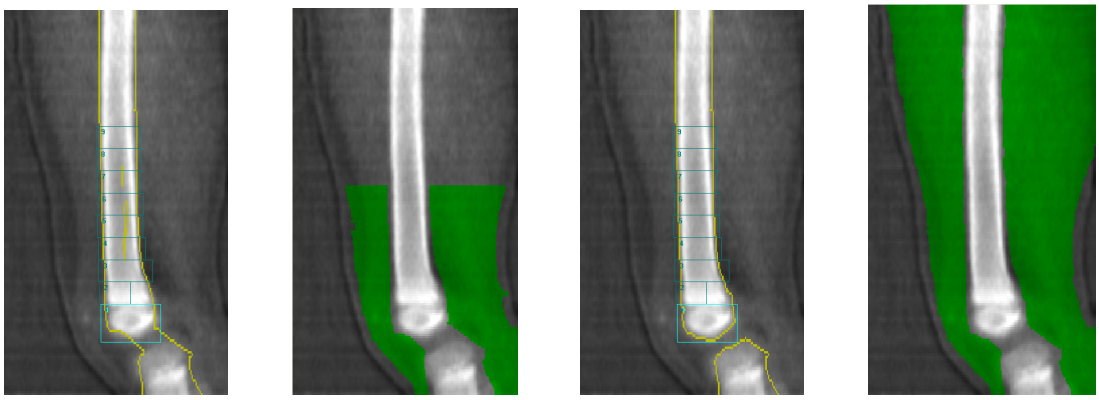

Figure 3.7 Results of manually editing the enCORE point typing. From right to left: Bone image with original edges detected by enCORE software; Original tissue detected by enCORE software; Bone images with edges edited by Megan Damcott; Tissue modified by Megan Damcott.

Table 3.1 Bone Mineral Densities (g/cm^2) of One Subject, Same Day, Same Leg. The 2nd through 4th columns represent the BMDs and the percent error with the default point typing of the EnCore software. Columns 5 through 7 demonstrate the BMDs and the percent error once the point typing has been edited by Megan Damcott. As can be seen, the percent errors after the point type editing has been done, fall within +-5%.

Region of Interest	Image 1: Prior to point type editing	Image 2: Prior to point type editing	% Error between BMD prior to editing	Image 1: After point type editing	Image 2: After point type editing	% Error between BMD after editing
2	0.739	0.713	3.52	0.738	0.716	2.98
3	0.575	0.583	-1.39	0.575	0.583	-1.39
4	0.585	0.564	3.59	0.582	0.558	4.12
5	0.584	0.582	0.34	0.575	0.568	1.22
6	0.535	0.572	-6.92	0.526	0.543	-3.23
7	0.559	0.564	-0.89	0.546	0.552	-1.10
8	0.570	0.537	5.79	0.546	0.532	2.56
9	0.641	0.581	9.36	0.605	0.579	4.30

The analysis to determine which factors have an impact on the precision of the present study concludes that factors relating to the point typing and algorithms in the enCORE software are the significant sources of error and can be corrected by manually editing the point typing, as is currently accepted in the clinical field. The analysis also provides analysis techniques appropriate for further consideration and investigation to increase the precision of DXA and allow multi-site studies or comparisons between studies.

3.4 Regions of Interest

Twelve custom ROIs were selected for this study. In preliminary analysis of the data, the three ROIs defined by Henderson et al. (2002) for the lateral distal femoral scanning procedure were used. These ROIs are not a 'gold' standard in the field, but they are becoming increasingly utilized in children as they are based upon the anatomical measure of the diameter of the femur and are speculated to not only account for differences in size between children, but also some degree of growth. As Figure 3.8 illustrates, the height of the Henderson et al. ROIs is twice the diameter of the mid-shaft of the femur. These regions are based upon normal children with the assumption that the ratio of the length and width of the femur are relatively constant throughout the subject population in question. As it is known that the ratio changes throughout childhood (Goulding et al. 1996) and children with CP have varying degrees of diminished longitudinal growth in the femur (Henderson et al. 2005), the ROIs were compared between subjects to ensure that they did cover the intended regions of bone postulated by Henderson et al. (2002)

within this study. As can be seen by the examples from three different subjects in Figure 3.8, the ROIs do encompass approximately the same regions between the subjects.

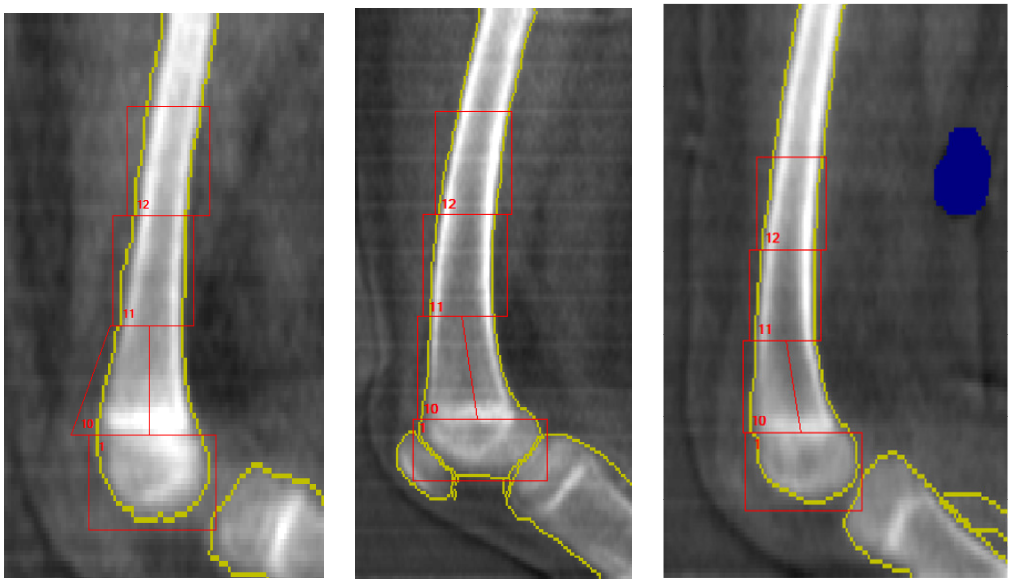

Figure 3.8 Three Henderson et al. regions of interest for three subjects. Regions 10 through 12 were based from the ROIs defined for the lateral distal scanning method by Henderson et al. 2002. As can be seen, the ROIs cover approximately the same regions between subjects as intended.

The ROIs in the femur mode of current DXA software use predefined ROIs which do not account for anatomical differences in bone size, do not allow for multiple ROIs to be investigated and only allow the mid-shaft or proximal femur to be investigated. Henderson et al. defined the three ROIs with the intention of the distal most ROI (Region 10 in this study) consisting of primarily trabecular bone, Region 11 consisting of the transitional region with a combination of trabecular and cortical bone (where femoral fractures are most prevalent in non-ambulant children) and Region 12 consisting primarily of cortical bone. Defining the ROIs in such a way allows the impact of the intervention to be considered in each type of bone separately. This is significant because as noted in the discussion of previous studies in Chapter 1, mechanical loading has been found to have significantly different impacts on trabecular and cortical bone. Further

examination of the pooled bone mineral densities in one representative subject's three ROIs (Figure 3.9) demonstrate that the BMD increases from Region 10 through 12. As the density of cortical bone is greater than trabecular and the ratio of cortical bone increases in the femur from the distal growth plate to the mid-shaft, the visual trends seen in Figure 3.9 are expected and suggest the ROIs cover the regions Henderson et al. intended.

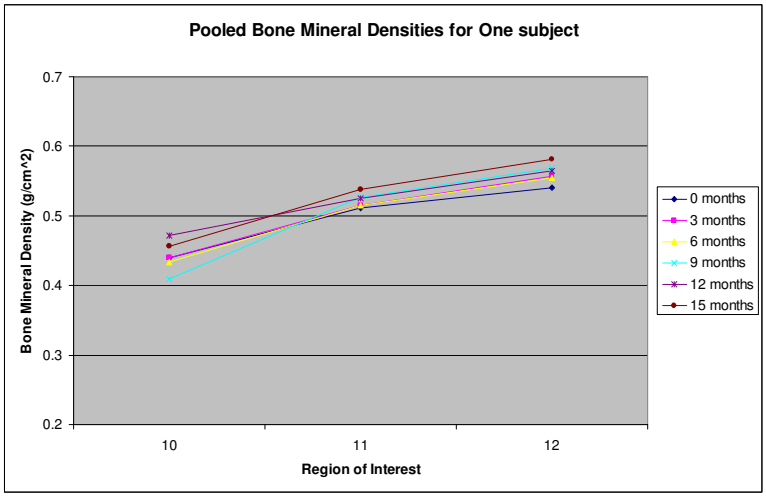

Figure 3.9 Pooled bone mineral densities for one representative subject (3 ROIs). The relative size of the three Henderson et al. (2002) ROIs mask the trends expected in bone mineral density in the distal femur. When compared to the trends in the one centimeter ROIs in Figure 3.10, it can be seen that the one centimeter ROIs more appropriately represent the trends of BMD in the region of fracture.

Figure 3.9 also demonstrates that the Henderson et al. (2002) ROIs can measure only the crude trends in trabecular and cortical bone within the distal femur. Therefore, in an effort to more thoroughly understand the trends occurring within the fracture region (primarily Region 11), a second group of novel ROIs were investigated in this study. Instead of deriving the height of each ROI from the ratio of femur length and width, each ROI had a constant height of one centimeter (chosen as the Henderson et al. ROIs ranged in height between two and three centimeters in this study). While the one centimeter

ROIs do not account for the static differences between the femur lengths of the subjects, nor do they account for longitudinal growth of the femur throughout the study, it was anticipated they would account for significant trends or changes the Henderson et al. ROIs may mask. As the area of interest for this study is the fracture region in the distal femur and this region does not move in relation to the growth plate, the one centimeter ROIs ensure that more thorough trends are investigated. The eight one centimeter ROIs extend through the metaphyseal region of the bone in all subjects where fractures are most prevalent and provide insight to trends which the Henderson et al. ROIs cannot provide due to the larger proportion of the femur covered by each of their ROIs. The pooled data of the one centimeter ROIs for one representative subject are plotted in Figure 3.10. As can be seen, the trends of BMD expected in the distal femur are more visible in the one centimeter ROIs (compared to those in Figure 3.9). The BMD decreases in Region 3 and 4 (where the cross-sectional diameter of the distal femur head is decreasing and a greater amount of trabecular bone exists due to longitudinal growth) as expected. The BMD then increases gradually through Regions 5 through 7 and begins to plateau in Regions 8 and 9, nearing the mid-shaft of the femur where the BMD should be relatively constant. As the trends within the distal femur are more appropriate in the one centimeter ROIs, this study analyzed both the Henderson et al. ROIs and the one centimeter ROIs to determine if the Henderson et al. ROIs do potentially mask trends in BMD, BMC and ROI area in growing children.

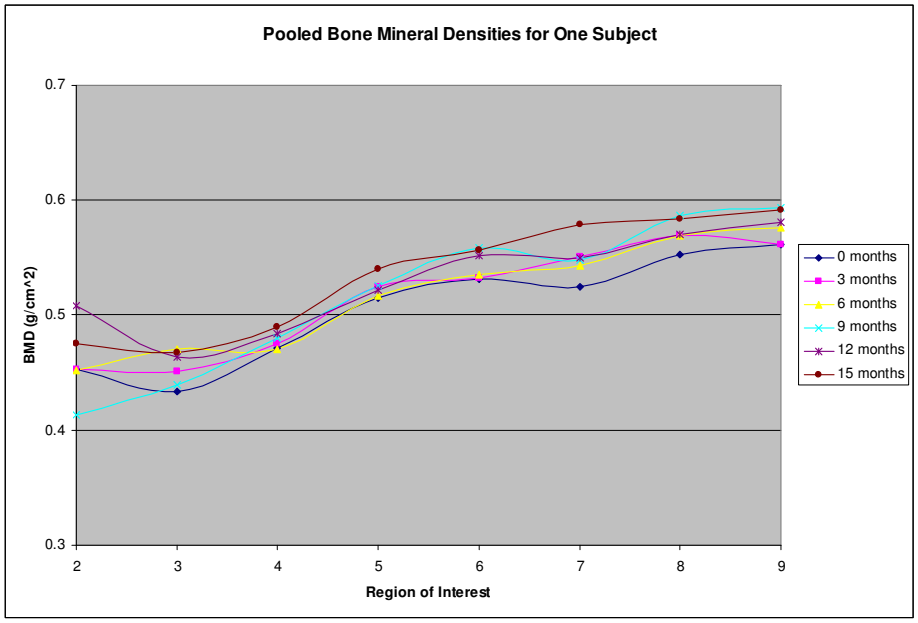

Figure 3.10 Pooled bone mineral densities for one representative subject (one cm ROIs). ROI 2 is located in the trabecular bone immediately above the distal growth plate with ROIs 3 through 9 aligned proximally into the mid-shaft of the femur. As expected, the BMD decreases in Region 3, where the distal femoral head is beginning to decrease in cross-sectional diameter (or 'neck in') and then increases until it nears a plateau in the mid-shaft area of Regions 8 and 9.

In the one centimeter ROIs, Region 1 was strictly a placement ROI to ensure proper placement of all other ROIs. The proximal edge of Region 1 was placed on the proximal edge of the distal growth plate in the distal femur (Figure 3.11). Regions 2 through 9 were all one centimeter in height with the distal most region (Region 2) placed in the same position relative to the growth plate as Region 10. Region 2 extended from the anterior edge of the distal lateral femur to half the width of the femur as in Region 10. Regions 3 through 9 extended across the full width of the femur. Region 2 was stacked on the proximal edge of Region 1 with Regions 3 through 9 then stacked proximally from the distal edge of the former region in numerical order. In this study, Regions 2 to 3 consist primarily of trabecular bone, Regions 4 through 7 consist of a combination of trabecular and cortical and Regions 8 and 9 consist of primarily cortical bone. Due to the difference in femoral lengths, these trends are not consistent for every subject but are

observed in the majority of subjects. This limitation will be further addressed in the discussion (Section 5.1).

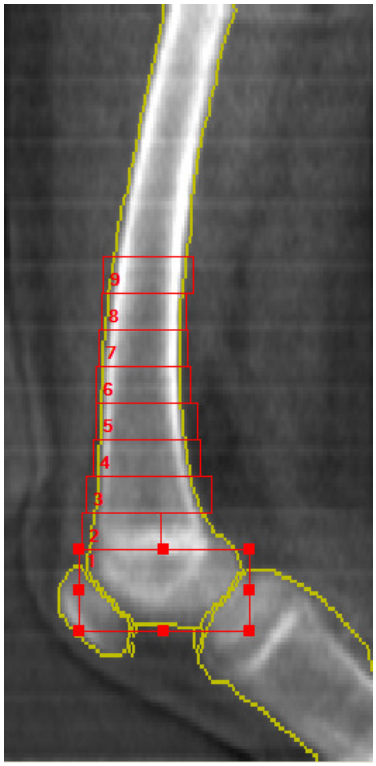

Figure 3.11 Eight one centimeter regions of interest. Region 2 begins at the proximal growth plate and extends one centimeter proximally. Regions 3 through 9 extend proximally from Region 2 in numerical order.

CHAPTER 4

ANALYSIS AND RESULTS

4.1 Introduction

Two dual-energy x-ray absorptiometry scans were obtained for each leg at each time interval and ROIs were placed in each scan using the method described in Section 3.4. As previously discussed, the preliminary analysis revealed that the precision of the scans was questionable. However, after completing the clinically accepted manual editing of the bone and tissue point-typing as described in Chapter 3, the mean error of this study (0.45%) has a variability of +/- 4.5%, which is within the accepted +/- 5%. Once the precision for this study was verified, the average BMD, BMC and ROI area were calculated for the same day/same leg scans. The right and left leg measurements were then pooled for each subject as established in the literature (Bailey et al. 1999, Bass et al. 1998 and Chad et al. 1999). The pooled BMD measurements of one representative subject are listed in Table 4.1 and plotted in Figure 3.10.

Table 4.1 Pooled Bone Mineral Densities for One Representative Subject

Region of Interest	Bone Mineral Density (g/cm^2)					
	0 months	3 months	6 months	9 months	12 months	15 months
2	0.453	0.453	0.452	0.413	0.509	0.475
3	0.433	0.451	0.471	0.439	0.464	0.467
4	0.472	0.475	0.470	0.480	0.484	0.490
5	0.515	0.525	0.517	0.526	0.522	0.540
6	0.531	0.532	0.536	0.559	0.552	0.557
7	0.525	0.551	0.543	0.548	0.550	0.579
8	0.553	0.570	0.569	0.587	0.571	0.584
9	0.562	0.562	0.576	0.594	0.581	0.592

The pooled data for each subject's measurements were normalized with respect to their baseline (0-month) measurements and multiplied by 100 to obtain the percent change. Formula 4.1 illustrates how the values were normalized for the BMD:

$$\text{Normalized BMD} = [(\text{BMD}(T) - \text{BMD}(\text{baseline})) / \text{BMD}(\text{baseline})]*100 \quad (4.1)$$

where T is the current elapsed time (in months) from the baseline measurement. The same normalization was used for the calculated BMCs and ROI areas as well. Figure 4.2 shows the percent change equivalents of the BMD values from Table 4.1 and Figure 3.10.

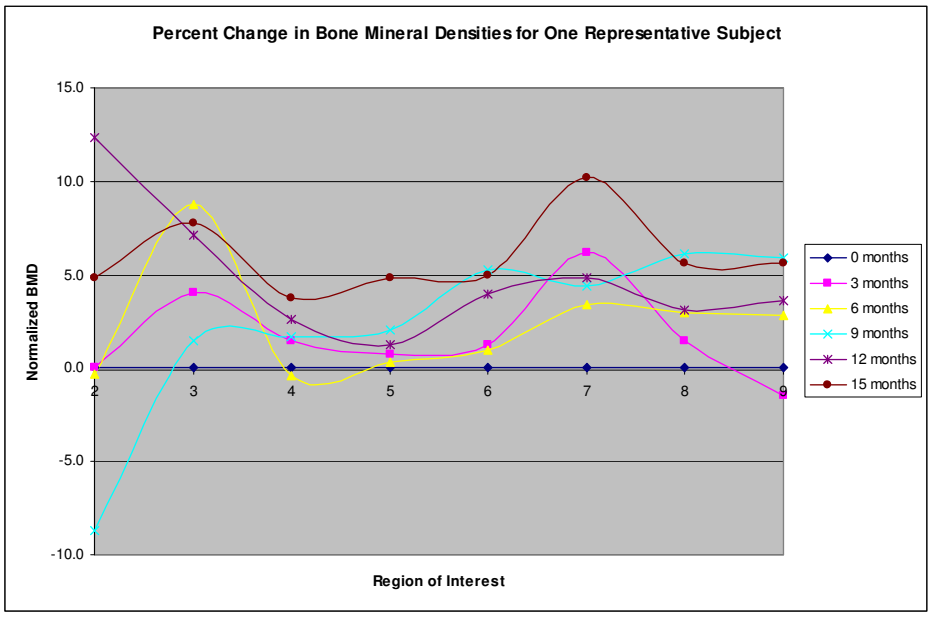

Figure 4.1 Percent changes in bone mineral densities for one representative subject.

Once the percent change values were calculated for each subject, the means of the percent change for each ROI were calculated in each standing intervention and each time period. As it is expected that the standing interventions increase BMD, BMC and ROI area, a one-tailed t-test was conducted to determine if the means of percent change were significantly greater than zero. This chapter describes the statistical methods used to analyze the data and the results of each group of ROIs.

4.2 Statistical Analysis

The statistical analysis of the data in this study must consider a number of factors and responses. The factors to consider were the standing intervention, the elapsed time and the ROI. The BMD, BMC and ROI area were each responses. The percent changes in BMD, BMC and ROI area were calculated as described in section 4.1. Two separate statistical analyses were completed: one encompassing the data of only the subjects who participated in the full 15 month study (Phase 1-3) and the other encompassing the data of all subjects participating in the first six months of the study (Phase 1).

4.2.1 Statistical Analysis of Full Fifteen Months (Phase 1 through Phase 3)

Analyses of the three ROIs defined by Henderson et al. and one centimeter ROIs were separated. The mean percent change of BMD, BMC and ROI area were calculated for each ROI in each standing intervention and elapsed time. Data from four subjects participating in the passive standing intervention and five in the dynamic were analyzed for a total n = 9. A 0.05 level of significance (α) was used.

4.2.2 Statistical Analysis of First Six Months (Phase 1)

Similar to section 4.2.1, analyses of the three ROIs defined by Henderson et al. and one centimeter ROIs were separated. The mean percent change of BMD was calculated for each ROI in each standing intervention and elapsed time. Data from six subjects participating in the passive standing intervention and seven in the dynamic were analyzed for a total n = 13. A 0.05 level of significance (α) was used.

4.3 Results for Full Fifteen Months of Study (Phase 1 through Phase 3)

4.3.1 Analysis of the Three Regions of Interest

The mean percent changes for each of the three Henderson et al. (2002) ROIs with respect to each standing intervention and elapsed time period are shown in Table 4.2. As the precision of this study is +-5%, the mean percent change must exceed this level to suggest changes. Any values which exceed the precision of the study are indicated with an asterisk (*). In the table, 'Dyn' and 'Pass' stand for the dynamic and passive standing interventions, respectively.

Table 4.2 Mean Percent Changes in Bone Mineral Density for Henderson et al. ROIs. As the precision of the study is +-5%, the mean percent change must exceed this magnitude to indicate changes in the time period considered. Any values which indicate significant changes are marked with an asterisk (*). Dyn: dynamic standing intervention. Pass: passive standing intervention.

ROI	MEAN PERCENT CHANGES IN TIME FOR BONE MINERAL DENSITY									
	3 months		6 months		9 months		12 months		15 months	
	Dyn	Pass	Dyn	Pass	Dyn	Pass	Dyn	Pass	Dyn	Pass
10	-1.56	-4.68	1.98	-3.98	-0.30	-7.07*	2.86	1.70	6.42*	-1.03
11	2.78	-0.35	4.80	0.83	3.60	-0.07	6.24*	4.25	7.62*	2.28
12	4.78	0.68	6.78*	0.48	5.96*	3.27	9.82*	1.53	7.70*	0.78

Figures 4.2 and 4.3 illustrate the individual visual trends associated with BMD for the dynamic and passive standing interventions, respectively, at each of the three Henderson et al. ROIs. In these figures, the average percent changes for BMD across all subjects participating in the specified intervention are graphed at 3-, 6-, 9-, 12- and 15-months. Similar to Table 4.2 above, the plots indicate that the dynamic standing intervention exceeds the +-5% precision level in the cortical bone of Region 12 after 6 months and the trabecular bone of Region 10 after 15 months. The mean percent changes in the passive standing intervention suggest that BMD is maintained throughout the study

as the values do not exceed the +-5% (with the exception of the 9-month BMD in Region 10, which could be explained as an outlier due to the small sample size).

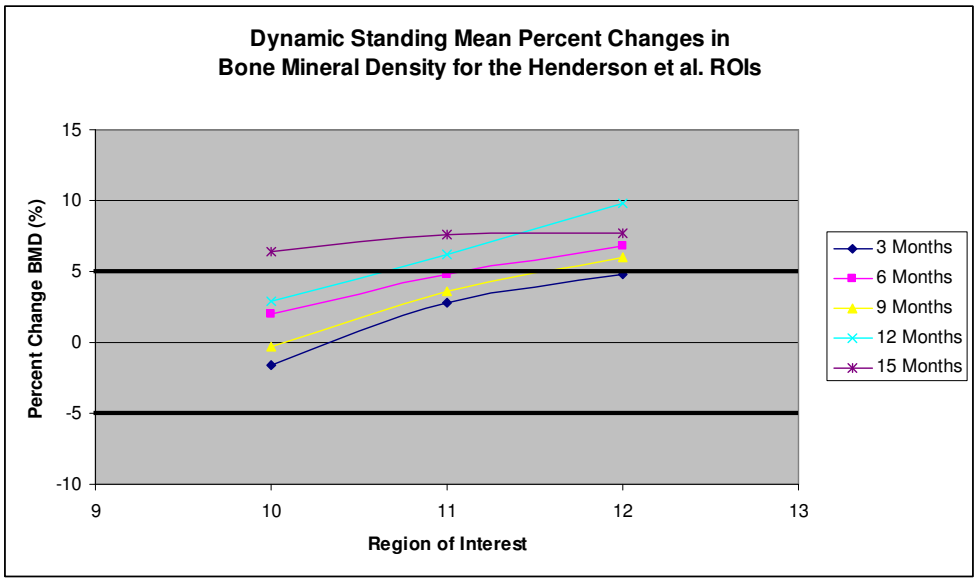

Figure 4.2 Mean percent change in bone mineral density (3 ROIs): dynamic standing. The mean percent changes in each of the three ROIs are plotted for 3-, 6-, 9-, 12-, and 15-months. The bold black lines at +- 5% indicate the precision of the study. Trends suggest that dynamic standing increases BMD after six months in the cortical bone of Region 12, with the nine month BMD measurements showing a trend to decrease after the passive standing phase (months 6 to 9). The trabecular bone of Region 10 suggests an increase after 15-months.

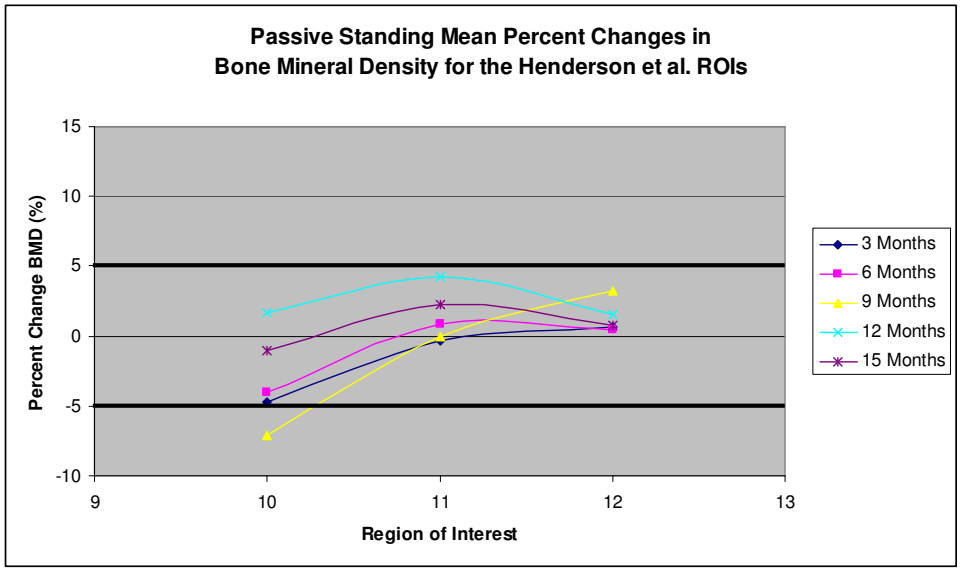

Figure 4.3 Mean percent change in bone mineral density (3 ROIs): passive standing. The mean percent changes in each of the three ROIs are plotted for 3-, 6-, 9-, 12-, and 15-months. The bold black lines at +- 5% indicate the precision of the study. Trends suggest that passive standing maintains BMD.

A closer inspection of the dynamic standing trends supports the potential of passive standing to maintain BMD. The trends in Figure 4.2 demonstrate an increased BMD in the dynamic standing intervention between the 3 and 6 month time period and again between the 9 and 15 month time period. However, during the period between 6 and 9 months, the BMD appears to only be maintained or potentially decrease to the baseline level. As this period included the passive standing during Phase 2 of the study, it would be expected that the BMD would be maintained as suggested by the trends shown in the passive standing intervention and thereby the maintenance of BMD during passive standing is further supported by the trends in the dynamic standing plot.

While trends may be visible in the tables and plots above, a statistical analysis of the data must be performed to verify whether the trends reach statistical significance. As the hypothesis of the study states that the dynamic standing intervention increases BMD,

a one-tailed t-test was performed to test if the mean percent changes were greater than 0. Table 4.3 displays the p-values. Any p-values which reach significance with α=0.05 are indicated with an asterisk (*). Although the visual trends suggest increases within the trabecular bone of Regions 10 and 11 after 12 months of dynamic standing, the statistical analysis reveals that the trends are not significant. However, the statistical analysis does confirm that the visual trends of increases in the cortical bone of Region 12 in dynamic standing are significant.

Table 4.3 P-values for Bone Mineral Density in the Henderson et al. ROIs. Any values which indicate significance above the 95% confidence level (α=0.05) are marked with an asterisk (*). Dyn: dynamic standing intervention. Pass: passive standing intervention.

ROI	**P-VALUES IN TIME FOR BONE MINERAL DENSITY**									
	3 months		6 months		9 months		12 months		15 months	
	Dyn	Pass	Dyn	Pass	Dyn	Pass	Dyn	Pass	Dyn	Pass
10	0.743	0.744	0.322	0.744	0.524	0.725	0.274	0.384	0.292	0.599
11	0.071	0.575	0.051	0.287	0.150	0.505	0.133	0.077	0.074	0.328
12	0.029*	0.346	0.016*	0.297	0.033*	0.066	0.018*	0.168	0.030*	0.417

While potential increases in the BMD of the trabecular bone were not determined to be statistically significant, improvement in the strength and health of the trabecular bone in the distal femur could be masked by underlying trends in the BMC and ROI area. Therefore, the trends within the BMC and ROI area were investigated in this study as well. Table 4.4 and Figures 4.4 and 4.5 illustrate the mean percent changes in BMC in each of the standing interventions over the duration of the study.

Table 4.4 Mean Percent Changes in Bone Mineral Content for Henderson et al. ROIs. As the precision of the study is +-5%, the mean percent change must exceed this magnitude to indicate changes in the time period considered. Any values which indicate significant changes are marked with an asterisk (*). Dyn: dynamic standing intervention. Pass: passive standing intervention.

ROI	MEAN PERCENT CHANGES IN TIME FOR BONE MINERAL CONTENT									
	3 months		6 months		9 months		12 months		15 months	
	Dyn	Pass	Dyn	Pass	Dyn	Pass	Dyn	Pass	Dyn	Pass
10	7.56*	2.45	12.26*	3.88	24.00*	21.47*	24.82*	32.85*	38.52*	15.33*
11	3.46	-0.10	7.38*	4.63	11.02*	9.43*	15.84*	11.30*	17.00*	11.40*
12	4.98	1.80	6.46*	7.23*	14.00*	12.73*	17.82*	12.58*	17.98*	12.35*

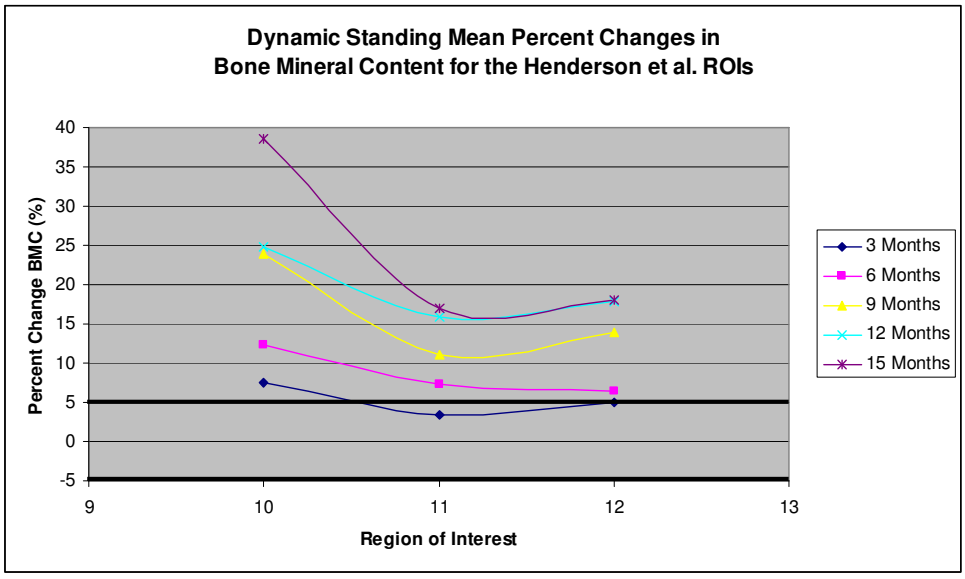

Figure 4.4 Mean percent change in bone mineral content (3 ROIs): dynamic standing. The mean percent change in each of the three ROIs are plotted for 3-, 6-, 9-, 12-, and 15-months. The bold black lines at +- 5% indicate the precision of the study. Trends suggest that dynamic standing increases BMC, with the greatest percent change in the trabecular bone of Region 10.

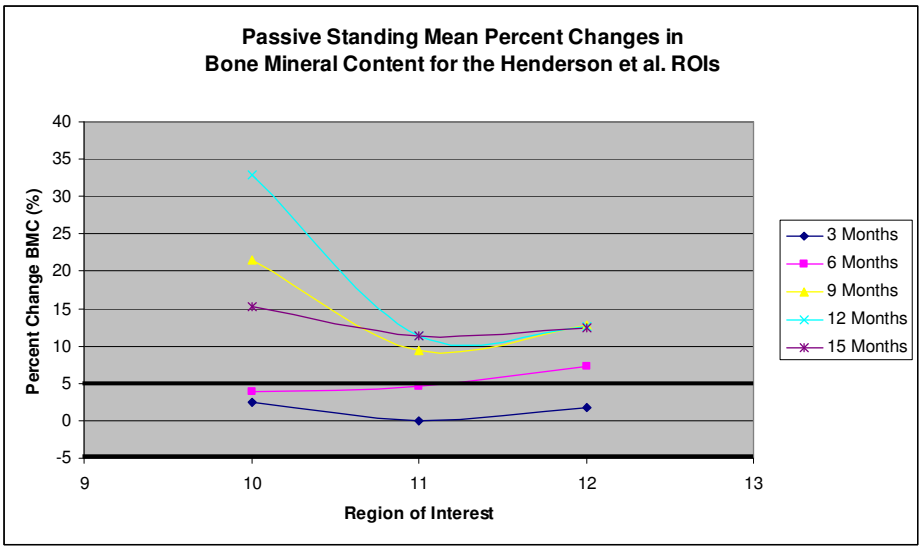

Figure 4.5 Mean percent change in bone mineral content (3 ROIs): passive standing. The mean percent change in each of the three ROIs are plotted for 3-, 6-, 9-, 12-, and 15-months. The bold black lines at +- 5% indicate the precision of the study. Trends suggest that passive standing increases BMC in trabecular bone at a greater rate than in cortical.

Increases in BMC are visible after 6 months of the dynamic standing intervention and 9 months of the passive standing intervention. Trends suggest the increases within the trabecular bone of Region 10, in both standing interventions, are greater than those in the cortical bone of Region 12. While the dynamic standing appears to increase BMC at a greater magnitude than the passive standing, a statistical analysis was performed and the p-values are listed in Table 4.5 below. The results of the statistical analysis support the visual trends of increased BMC in the cortical bone after 9 months, but do not consistently conclude significant changes within the trabecular bone as the means and graphs above suggest.

Table 4.5 P-values for Bone Mineral Content in the Henderson et al. ROIs. Any values which indicate significance above the 95% confidence level (α=0.05) are marked with an asterisk (*). Dyn: dynamic standing intervention. Pass: passive standing intervention.

ROI	P-VALUES IN TIME FOR BONE MINERAL CONTENT									
	3 months		6 months		9 months		12 months		15 months	
	Dyn	Pass	Dyn	Pass	Dyn	Pass	Dyn	Pass	Dyn	Pass
10	0.263	0.406	0.154	0.348	0.125	0.021*	0.110	0.060	0.083	0.194
11	0.106	0.533	0.067	0.031*	0.048*	0.027*	0.044*	0.068	0.057	0.101
12	0.050*	0.232	0.051	0.083	0.028*	0.005*	0.015*	0.047*	0.023*	0.062

The mean percent changes in ROI area for each ROI and each standing intervention are listed in Table 4.6 and plotted in Figures 4.6 and 4.7. The areas of the trabecular bone in Region 10 increase throughout the study. Areas within Regions 11 and 12 appear to increase in both standing interventions at the same magnitude after 9 months.

Table 4.6 Mean Percent Changes in Region of Interest Area for Henderson et al. ROIs. As the precision of the study is +-5%, the mean percent change must exceed this magnitude to indicate changes in the time period considered. Any values which indicate significant changes are marked with an asterisk (*). Dyn: dynamic standing intervention. Pass: passive standing intervention.

ROI	MEAN PERCENT CHANGE IN TIME FOR REGION OF INTEREST AREA									
	3 months		6 months		9 months		12 months		15 months	
	Dyn	Pass	Dyn	Pass	Dyn	Pass	Dyn	Pass	Dyn	Pass
10	13.58*	7.73*	10.40*	8.43*	23.70*	32.67*	20.72*	29.93*	28.3*	17.53*
11	0.70	0.20	2.48	4.05	6.94*	9.73*	8.54*	8.68*	9.56*	7.98*
12	0.24	1.20	0.36	6.60*	7.34*	9.17*	7.32*	10.82*	7.68*	12.38*

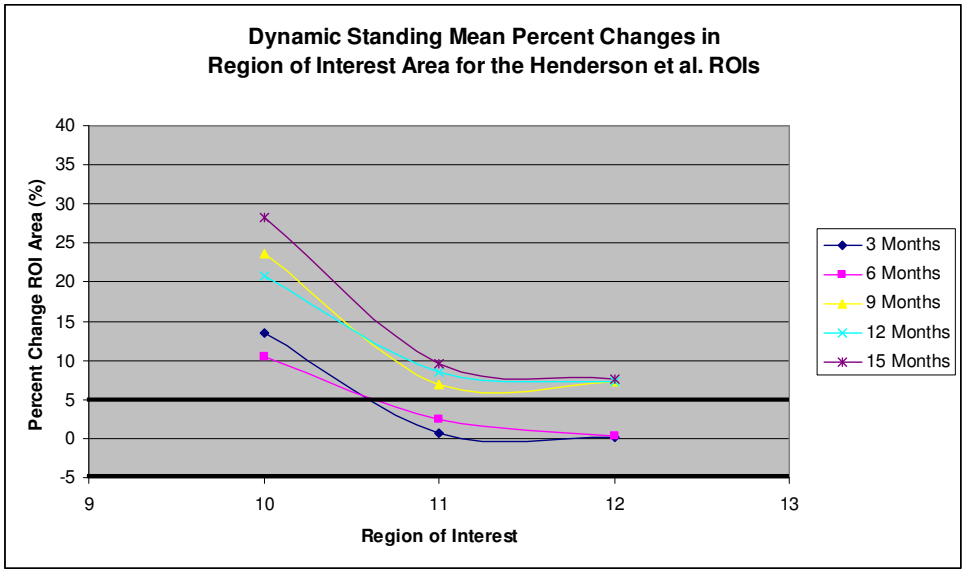

Figure 4.6 Mean percent change in area (3 ROIs): dynamic standing. The mean percent change in each of the three ROIs are plotted for 3-, 6-, 9-, 12-, and 15-months. The bold black lines at +- 5% indicate the precision of the study. Trends suggest area increases. However, this increase is approximately on the same magnitude as the increase in the trends associated with passive standing.

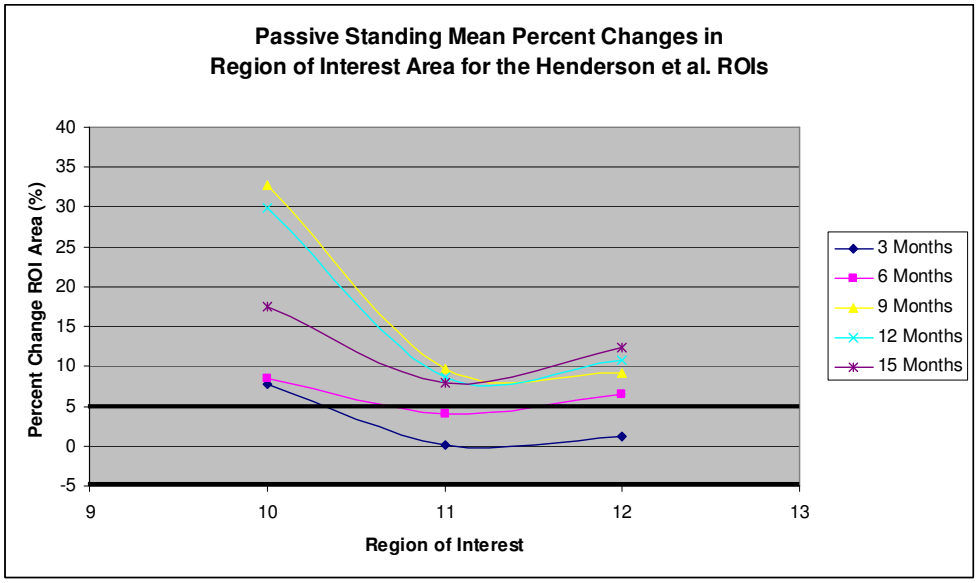

Figure 4.7 Mean percent change in area(3 ROIs): passive standing. The mean percent change in each of the three ROIs are plotted for 3-, 6-, 9-, 12-, and 15-months. The bold black lines at +- 5% indicate the precision of the study. Trends suggest area increases. However, this increase is on approximately the same magnitude as the increase in the trends associated with dynamic standing.

To determine whether the increases in ROI area between the two standing interventions are on the same magnitude, a statistical analysis was performed. The resulting p-values are listed in Table 4.7. Similar to the statistical significance determined in the BMC values for the Henderson et al. ROIs, the statistical analysis does not support the apparent visual trends in ROI area within the trabecular bone of Region 10. The statistical analysis also does not support the apparent trends seen within the means and plots which support increases in both the dynamic and passive standing interventions on cortical bone. The increases in ROI area with respect to the cortical bone in the passive standing were determined to be significant but the dynamic standing was not. While the visual inspection suggests these trends should yield the same statistical significance, the fact that the dynamic standing p-values are approaching this study's 95% confidence interval suggests that the small population size in this study could be the explanation of the statistical difference.

Table 4.7 P-values for Region of Interest Area in the Henderson et al. ROIs. Any values which indicate significance above the 95% confidence level (α=0.05) are marked with an asterisk (*). Dyn: dynamic standing intervention. Pass: passive standing intervention.

ROI	**P-VALUES IN TIME FOR REGION OF INTEREST AREA**									
	3 months		6 months		9 months		12 months		15 months	
	Dyn	Pass	Dyn	Pass	Dyn	Pass	Dyn	Pass	Dyn	Pass
10	0.102	0.179	0.130	0.172	0.094	0.046*	0.070	0.041*	0.056	0.120
11	0.333	0.446	0.125	0.080	0.039*	0.040*	0.055	0.060	0.059	0.035*
12	0.372	0.174	0.383	0.101	0.044*	0.001*	0.071	0.045*	0.089	0.018*

4.3.2 Analysis of the One Centimeter Regions of Interest

With the trends and statistics in the three Henderson et al. (2002) ROIs suggesting significantly different impacts of the standing interventions on trabecular and cortical bone, novel one centimeter ROIs were used to investigate the underlying trends in the fracture region of the distal femur (Region 11). The mean percent changes in each ROI are listed in Table 4.8 and the trends in dynamic and passive standing are plotted in Figures 4.8 and 4.9, respectively. Similar to the Henderson et al. ROIs, the trends suggest that dynamic standing increases the BMD in the cortical bone region after 3 months. The trends also show the same maintenance or potential decrease after the passive standing phase between months 6 and 9.

Table 4.8 Mean Percent Changes in Bone Mineral Density for One Centimeter Regions of Interest. As the precision of the study is +-5%, the mean percent change must exceed this magnitude to indicate changes in the time period considered. Any values which indicate significant changes are marked with an asterisk (*). Dyn: dynamic standing intervention. Pass: passive standing intervention.

ROI	MEAN PERCENT CHANGE IN TIME FOR BONE MINERAL DENSITY									
	3 months		6 months		9 months		12 months		15 months	
	Dyn	Pass	Dyn	Pass	Dyn	Pass	Dyn	Pass	Dyn	Pass
2	0.58	-3.98	4.80	-6.35	-0.38	-12.1	4.16	1.23	8.58*	-2.65
3	1.30	-6.33	7.18*	-0.50	1.28	-5.57	4.30	2.48	7.72*	0.58
4	1.60	-3.80	2.90	-2.05	-0.14	-2.9	3.26	2.13	6.18*	0.20
5	1.76	-0.33	4.98	1.03	2.52	-2.87	5.82*	2.88	7.22*	2.75
6	3.52	0.45	5.24*	-1.48	3.64	0.80	5.44*	2.33	7.12*	2.63
7	3.34	1.93	5.68*	-1.63	3.06	-0.30	6.70*	1.38	6.74*	0.90
8	5.42*	0.5	7.24*	-0.65	5.68*	3.10	7.52*	1.03	7.68*	0.18
9	5.76*	2.08	8.34*	1.08	6.84*	2.23	9.84*	1.65	9.20*	0.58

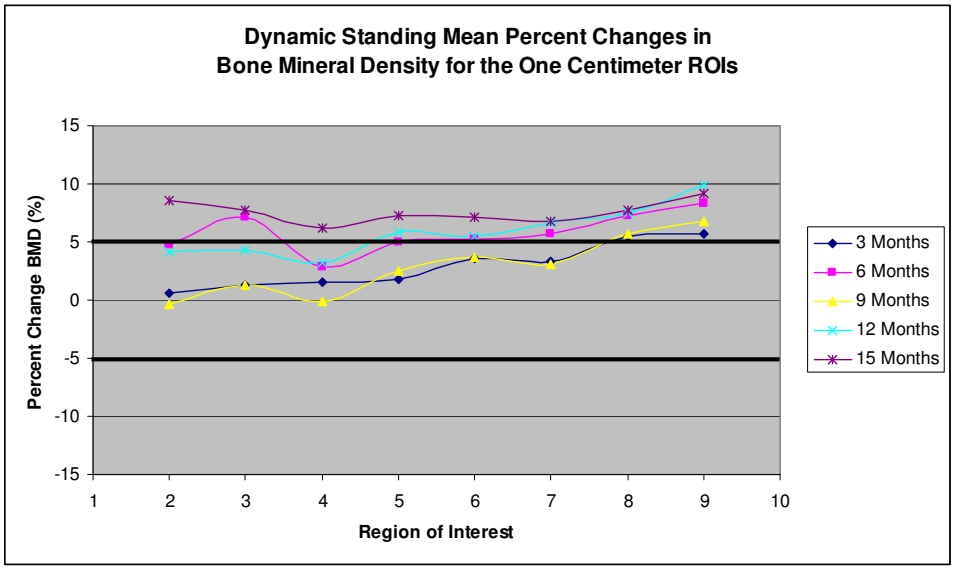

Figure 4.8 Mean percent change in bone mineral density (one cm ROIs): dynamic standing. The mean percent change in each of the one centimeter ROIs are plotted for 3-, 6-, 9-, 12-, and 15-months. The bold black lines at +- 5% indicate the precision of the study. Trends suggest that dynamic standing increases BMD in the cortical bone region after 3 months. Trabecular bone increased at 15 months. Similar to the trends in the Henderson et al. ROIs, the trends in the one cm ROIs suggest that BMD was maintained or potentially decreased during the passive standing phase between months 6 and 9.

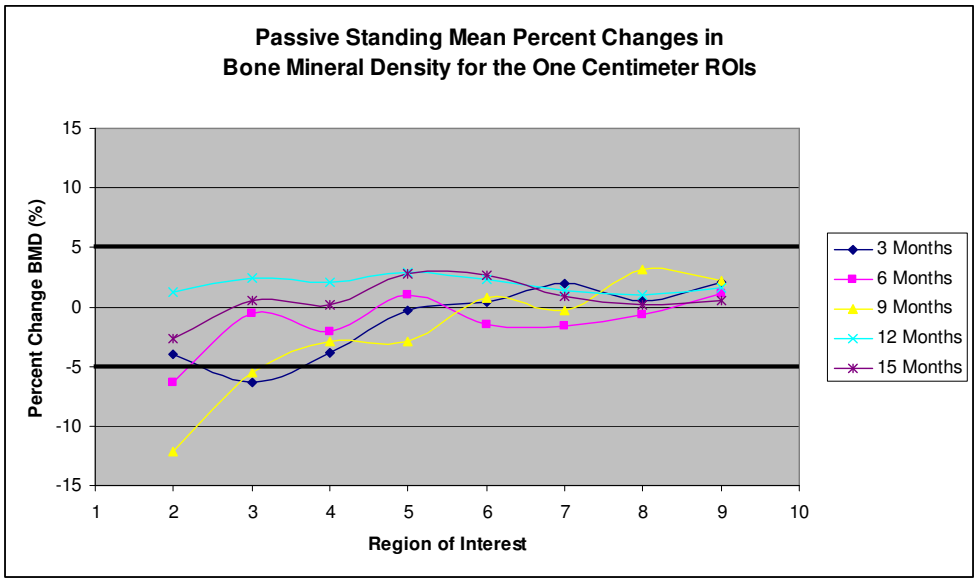

Figure 4.9 Mean percent change in bone mineral density (one cm ROIs): passive standing. The mean percent change in each of the one centimeter ROIs are plotted for 3-, 6-, 9-, 12-, and 15-months. The bold black lines at +- 5% indicate the precision of the study. Trends suggest that the passive standing maintains BMD at the baseline level.

A statistical analysis of the one centimeter ROIs verified the expectation that these ROIs could provide insight the Henderson et al. ROIs could not. The p-values (Table 4.9) for the BMD in the one centimeter ROIs reveal significance in the trends similar to those seen visually in the means and plots. Statistical analysis of the Henderson et al. ROIs determined that significant differences occurred only in the cortical bone region with respect to the mean percent changes in BMD of dynamic standing (approximately Regions 8 and 9 in the table below). Significant differences were not found in Region 11 as this region is a mixture of cortical and trabecular bone and encompasses too great an area to distinguish the trends within the fracture region demonstrated in the one centimeter ROIS below (Regions 4 through 7).

Table 4.9 P-values for Bone Mineral Density in the One Centimeter ROIs. Any values which indicate significance above the 95% confidence level (α=0.05) are marked with an asterisk (*). Dyn: dynamic standing intervention. Pass: passive standing intervention.

ROI	**P-VALUES IN TIME FOR BONE MINERAL DENSITY**									
	3 months		6 months		9 months		12 months		15 months	
	Dyn	Pass	Dyn	Pass	Dyn	Pass	Dyn	Pass	Dyn	Pass
2	0.337	0.757	0.143	0.862	0.545	0.810	0.177	0.420	0.226	0.714
3	0.263	0.812	0.008*	0.526	0.305	0.659	0.114	0.358	0.175	0.455
4	0.291	0.832	0.211	0.656	0.517	0.614	0.254	0.371	0.133	0.487
5	0.185	0.591	0.085	0.382	0.295	0.613	0.176	0.337	0.100	0.339
6	0.127	0.401	0.071	0.765	0.120	0.433	0.089	0.296	0.028*	0.303
7	0.054	0.222	0.011*	0.766	0.107	0.534	0.033*	0.354	0.023*	0.428
8	0.025*	0.272	0.013*	0.658	0.038*	0.092	0.016*	0.141	0.028*	0.477
9	0.018*	0.156	0.016*	0.156	0.021*	0.181	0.001*	0.072	0.021*	0.402

As in the section above, the trends within the BMC and ROI area were investigated in the one centimeter ROIs to determine if any underlying trends in the BMC or ROI area were masking trends in BMD. Tables 4.10 and 4.11 list the mean percent changes for BMC and ROI area, respectively. Trends in the BMC of the trabecular and cortical bone with respect to dynamic standing suggested increases after 6 months. For passive standing, the increases began at 9 months. Trends in ROI area demonstrated

increases in the trabecular bone regions in both standing interventions at 9 months and cortical bone at 12 months. Figures 4.10 through 4.13 below visually demonstrate the trends in BMC and ROI area.

Table 4.10 Mean Percent Changes in Bone Mineral Content for One Centimeter ROIs. As the precision of the study is +-5%, the mean percent change must exceed this magnitude to indicate changes in the time period considered. Any values which indicate significant changes are marked with an asterisk (*). Dyn: dynamic standing intervention. Pass: passive standing intervention.

ROI	MEAN PERCENT CHANGE IN TIME FOR BONE MINERAL CONTENT									
	3 months		6 months		9 months		12 months		15 months	
	Dyn	Pass	Dyn	Pass	Dyn	Pass	Dyn	Pass	Dyn	Pass
2	9.84*	-1.00	12.04*	-4.0	15.30*	-2.13	19.56*	22.10*	30.58*	4.63
3	1.64	-1.45	8.90*	0.25	8.40*	10.33*	10.62*	13.28*	18.52*	8.50*
4	2.20	-0.73	6.72*	-0.33	4.90	8.93*	9.96*	8.60*	15.24*	5.53*
5	1.78	1.38	6.86*	3.03	5.76*	5.13*	12.26*	9.75*	13.96*	8.25*
6	5.18*	2.28	8.58*	1.40	9.22*	7.30*	13.66*	8.20*	15.68*	7.70*
7	4.46	4.65	6.74*	3.43	10.00*	4.10	13.30*	9.73*	13.74*	9.18*
8	4.18	1.50	7.78*	2.55	12.02*	7.37*	13.12*	7.73*	13.62*	7.68*
9	6.16*	2.48	9.46*	4.93	12.28*	7.03*	14.74*	7.00*	16.76*	8.43*

Table 4.11 Mean Percent Changes in Region of Interest Area for One Centimeter ROIs. As the precision of the study is +-5%, the mean percent change must exceed this magnitude to indicate changes in the time period considered. Any values which indicate significant changes are marked with an asterisk (*). Dyn: dynamic standing intervention. Pass: passive standing intervention.

ROI	MEAN PERCENT CHANGE IN TIME FOR REGION OF INTEREST AREA									
	3 months		6 months		9 months		12 months		15 months	
	Dyn	Pass	Dyn	Pass	Dyn	Pass	Dyn	Pass	Dyn	Pass
2	7.82*	3.25	6.34*	2.25	15.16*	27.77*	12.98*	11.80*	14.12*	7.30*
3	1.28	4.53	3.28	2.15	6.96*	19.70*	6.38*	10.75*	4.80	7.58*
4	0.72	3.25	3.22	1.75	5.04*	13.37*	6.20*	6.28*	8.42*	5.15*
5	0.28	1.35	2.48	1.85	3.18	10.50*	5.96*	6.35*	6.28*	5.03*
6	1.00	-0.40	2.18	2.78	4.88	6.13*	6.56*	5.70*	7.74*	5.00
7	0.60	2.63	0.74	5.08*	6.22*	3.67	5.88*	8.25*	6.00*	7.58*
8	-1.06	0.43	0.20	2.80	5.02*	3.97	4.58	6.15*	5.10*	7.05*
9	-0.18	0.45	1.22	3.88	4.74	4.43	8.46*	5.3*	6.30*	7.9*

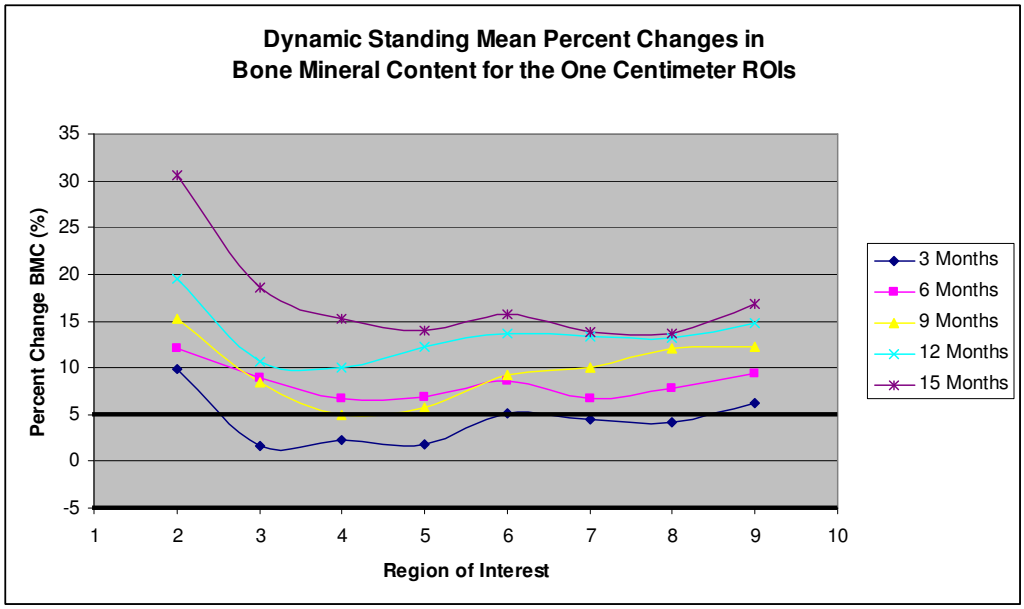

Figure 4.10 Mean percent change in bone mineral content (one cm ROIs): dynamic standing.The mean percent change in each of the one centimeter ROIs are plotted for 3-, 6-, 9-, 12-, and 15-months. The bold black lines at +- 5% indicate the precision of the study. Trends suggest that dynamic standing increases BMC, with the greatest percent change in the trabecular bone.

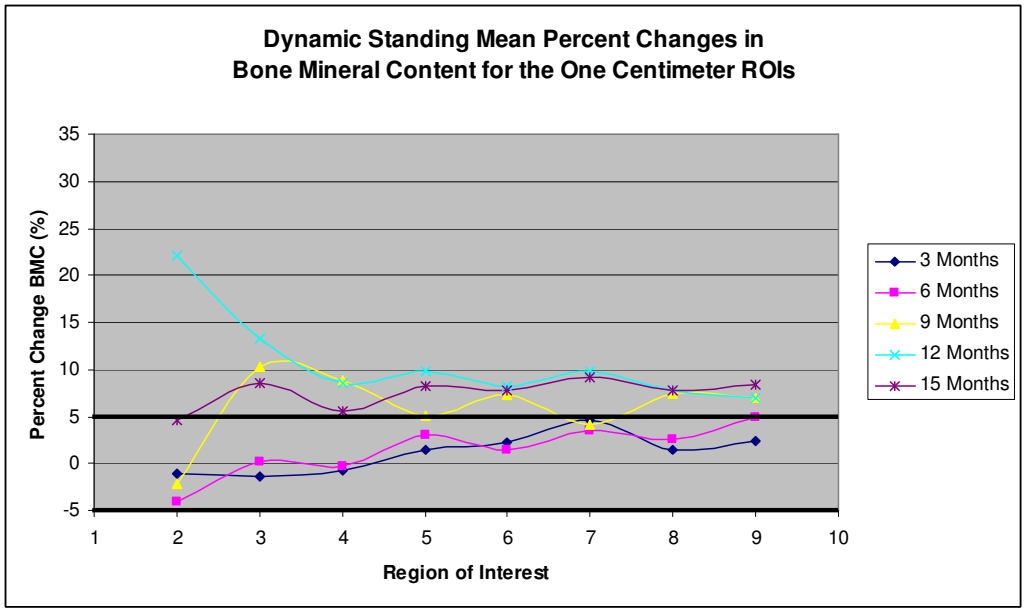

Figure 4.11 Mean percent change in bone mineral content (one cm ROIs): passive standing. The mean percent change in each of the one centimeter ROIs are plotted for 3-, 6-, 9-, 12-, and 15-months. The bold black lines at +- 5% indicate the precision of the study. The trends suggest that BMC increases after 9 months.

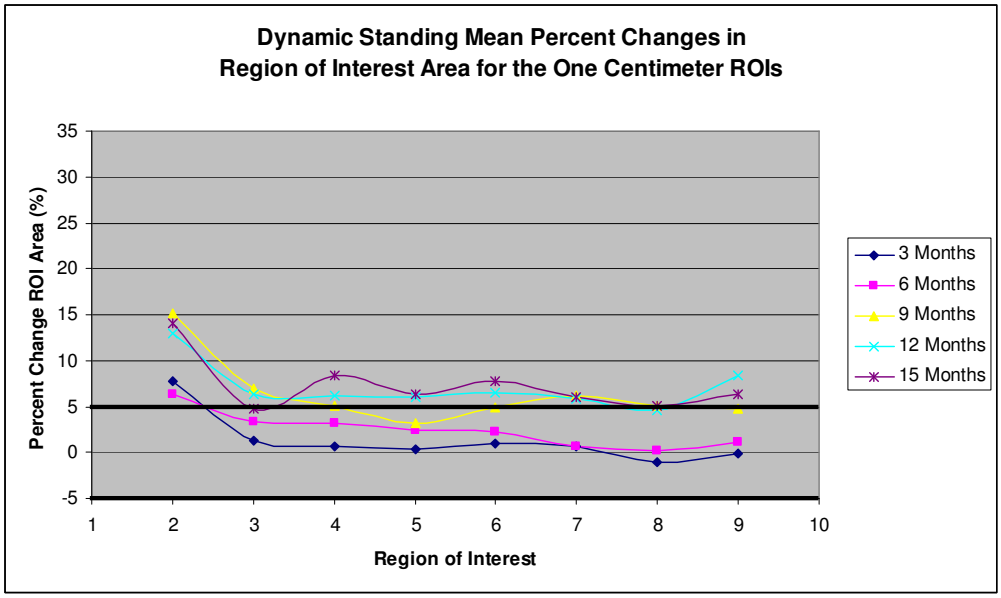

Figure 4.12 Mean percent change in area (one cm ROIs): dynamic standing. The mean percent change in each of the one centimeter ROIs are plotted for 3-, 6-, 9-, 12-, and 15-months. The bold black lines at +- 5% indicate the precision of the study. Trends suggest area increases at 12 months. However, this increase is on the same magnitude as the increase in the trends associated with passive standing.

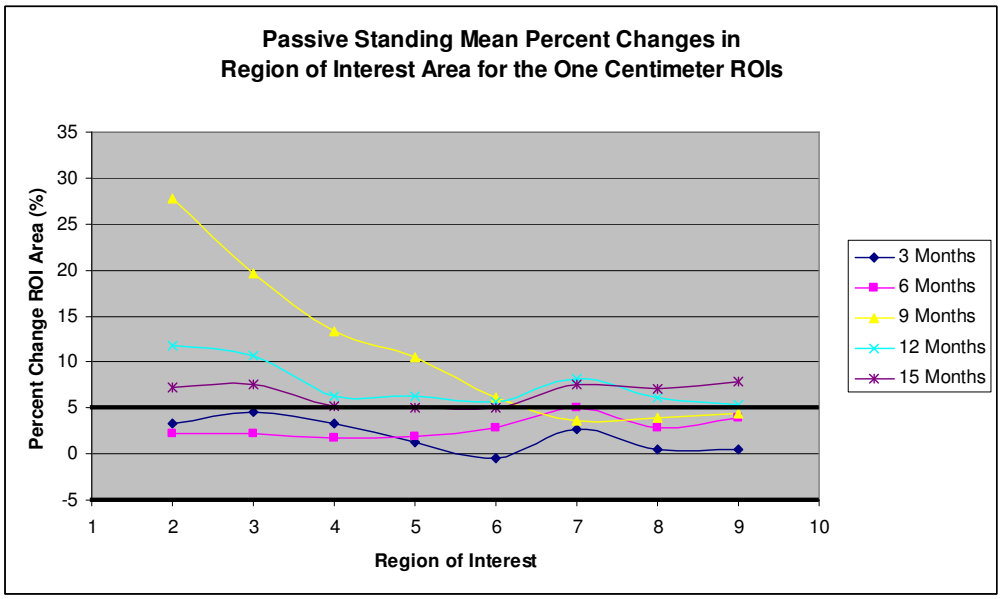

Figure 4.13 Mean percent change in area (one cm ROIs): passive standing. The mean percent change in each of the one centimeter ROIs are plotted for 3-, 6-, 9-, 12-, and 15-months. The bold black lines at +- 5% indicate the precision of the study. Trends suggest area increases at 12 months. However, this increase is on the same magnitude as the increase in the trends associated with dynamic standing.

Tables 4.12 and 4.13 list the p-values for the BMC and ROI area, respectively. Statistical significance was seen in the cortical region with respect to dynamic standing. This is similar to the resulting p-values in the Henderson et al. ROIs. Trends in ROI area suggest that the increases began to occur at 9 months. While, the trends within the ROI area are not consistent in either standing intervention, and therefore make it difficult to determine a concrete impact from the intervention, their unpredictability suggests that changes in the ROI area are dependent upon a factor other than the standing intervention.

Table 4.12 P-values for Bone Mineral Content in the One Centimeter ROIs. Any values which indicate significance above the 95% confidence level (α=0.05) are marked with an asterisk (*). Dyn: dynamic standing intervention. Pass: passive standing intervention.

ROI	**P-VALUES IN TIME FOR BONE MINERAL CONTENT**									
	3 months		6 months		9 months		12 months		15 months	
	Dyn	Pass	Dyn	Pass	Dyn	Pass	Dyn	Pass	Dyn	Pass
2	0.066	0.567	0.088	0.721	0.103	0.556	0.066	0.097	0.066	0.327
3	0.221	0.582	0.066	0.486	0.084	0.065	0.027*	0.086	0.076	0.145
4	0.274	0.566	0.114	0.528	0.164	0.098	0.056	0.132	0.066	0.216
5	0.281	0.230	0.121	0.197	0.164	0.279	0.055	0.122	0.061	0.140
6	0.063	0.099	0.014*	0.277	0.017*	0.117	0.009*	0.087	0.005*	0.109
7	0.070	0.098	0.019*	0.104	0.014*	0.288	0.011*	0.058	0.024*	0.091
8	0.112	0.051	0.031*	0.096	0.018*	0.091	0.019*	0.063	0.054	0.082
9	0.022*	0.048*	0.008*	0.047*	0.002*	0.045*	0.013*	0.084	0.026*	0.048*

Table 4.13 P-values for Region of Interest Area in the One Centimeter ROIs. Any values which indicate significance above the 95% confidence level (α=0.05) are marked with an asterisk (*). Dyn: dynamic standing intervention. Pass: passive standing intervention.

ROI	**P-VALUES IN TIME FOR REGION OF INTEREST AREA**									
	3 months		6 months		9 months		12 months		15 months	
	Dyn	Pass	Dyn	Pass	Dyn	Pass	Dyn	Pass	Dyn	Pass
2	7.82*	3.25	6.34*	2.25	15.16*	27.77*	12.98*	11.80*	14.12*	7.30*
3	1.28	4.53	3.28	2.15	6.96*	19.70*	6.38*	10.75*	4.80	7.58*
4	0.72	3.25	3.22	1.75	5.04*	13.37*	6.20*	6.28*	8.42*	5.15*
5	0.28	1.35	2.48	1.85	3.18	10.50*	5.96*	6.35*	6.28*	5.03*
6	1.00	-0.40	2.18	2.78	4.88	6.13*	6.56*	5.70*	7.74*	5.00
7	0.60	2.63	0.74	5.08*	6.22*	3.67	5.88*	8.25*	6.00*	7.58*
8	-1.06	0.43	0.20	2.80	5.02*	3.97	4.58	6.15*	5.10*	7.05*
9	-0.18	0.45	1.22	3.88	4.74	4.43	8.46*	5.3*	6.30*	7.9*

4.4 Results for First Six Months

The first six months of data for the individuals who participated in the full 15 month study was included in the analyses in Section 4.3. However, there were four children who participated in the first six months, but were unable to complete the full 15 months. An analysis of the first six months of data for all 13 subjects was performed and the p-values are listed in Table 4.14.

Table 4.14 P-values for Bone Mineral Density for the First Six Months. The tables show the p-values for the first six months with 13 of the original subjects. A comparison between these tables and the respective tables in Section 4.3, demonstrate how an additional four subjects increases the power of the statistical analysis. Any values which indicate significance above the 95% confidence level (α=0.05) are marked with an asterisk (*). Dyn: dynamic standing intervention. Pass: passive standing intervention.

ROI	P-VALUES IN TIME			
	3 months		6 months	
	Dyn	Pass	Dyn	Pass
10	0.763	0.755	0.189	0.832
11	0.034*	0.606	0.017*	0.182
12	0.008*	0.309	0.002*	0.085

ROI	P-VALUES IN TIME			
	3 months		6 months	
	Dyn	Pass	Dyn	Pass
2	0.764	0.673	0.164	0.903
3	0.190	0.830	0.009*	0.531
4	0.267	0.863	0.116	0.584
5	0.132	0.495	0.046*	0.288
6	0.091	0.482	0.042*	0.707
7	0.011*	0.140	0.001*	0.582
8	0.011*	0.070	0.002*	0.598
9	0.006*	0.096	0.003*	0.034*

CHAPTER 5

DISCUSSION AND CONCLUSIONS

5.1 Discussion

According to current research in bone health and the impact of mechanical loading in immobilized populations, this study hypothesized that incorporating a dynamic standing intervention which provided reciprocal loading, mimicking walking, into the therapeutic protocols of non-ambulant children would improve BMD at a greater rate than the current passive standing intervention. The results of the study conclude that dynamic standing does statistically increase BMD, while passive standing maintains BMD.

As discussed in Chapter 3, the precision of this study is 5%. Therefore, in order for any significant increases to be determined, the potential change must be greater than 5%. Bone mineral density increases due to the dynamic standing exceed the 5% precision within the proximal ROIs. This suggests that dynamic standing has the ability to increase BMD in cortical bone. Passive standing BMD trends do not exceed the 5% precision level, suggesting that BMD is maintained with passive standing. The larger, consistent reciprocal loading provided by dynamic standing appears more effective than the small, intermittent shifting experienced during passive standing.

The apparent trends within the BMD of the subjects participating in the dynamic standing intervention further support the suggestion of passive standing's ability to maintain the BMD. In Phase 2 of this study, all subjects stood passively between the 6 and 9 month time period. The statistical analysis of the effect elapsed time has on BMD for dynamic standing show an increased BMD in the cortical bone within the first 6

months. The BMD is then maintained (with a potential trend suggesting that the BMD actually decreases towards the baseline BMD measures) for months 6 through 9, before another increase is seen in months 12 and 15. The maintenance of BMD in the subjects in dynamic standing throughout the mid-portion of the study when the subjects are standing passively, but increases in BMD on either end of the study when they are standing in the dynamic stander strongly supports the suggestion that a passive standing intervention is able to maintain baseline BMD values. As ethical and logistical reasons prevented this study from collecting longitudinal data on non-ambulatory children with no weight-bearing intervention, the BMD trends seen within the dynamic stander are important. Without the data on subjects with no intervention, it cannot be determined if passive standing is an improvement over no weight-bearing. However, the trends in the dynamic standing population, coupled with work from previous studies which demonstrate decreased BMD during immobilization and bed rest (Heer 2007), do support the benefit of passive standing in maintaining BMD.

Interestingly, two other trends in BMD can be seen within the one centimeter ROIs that are not apparent within the Henderson et al. ROIs. The first apparent trend to note is which ROIs reach statistical significance in each time period. In the dynamic standing intervention, the cortical bone in Region 8 and 9 is statistically significant throughout the duration of the study. Region 7 becomes statistically significant in month 6 (after three months of dynamic standing), is no longer statistically significant in month 9 (after 3 months of passive standing) and once again becomes significant in month 12 (after another three month period of dynamic standing). With Region 7 reaching statistical significance in month 12, Region 6 becomes statistically significant in month

15. This suggests that modeling is greatest at the cortical region nearing the mid-shaft of the diaphysis and is temporally shifting distally from the diaphyseal region, through the metaphyseal region, towards the distal growth plate; increasing the ratio of the cortical to trabecular bone within the metaphyseal region.

The second apparent trend indirectly supports this first trend as it appears the increase in BMD within the dynamic standing begins to plateau. Regions 7, 8 and 9 gradually increase in BMD in months 3 and 6, decrease in month 9 following the passive standing phase, before increasing again in month 12. At 15 months, the increase is sustained from month 12, suggesting that the regions have reached a plateau. This could be due to the conservative nature of the loading being applied as discussed later in this section. The appearance of these trends within the one centimeter ROIs, but not the Henderson et al. ROIs, suggest that the overall size of the Henderson et al. ROIs do mask underlying trends within the regions of fracture in growing children.

Both standing interventions demonstrated the potential to increase BMC in the cortical bone region, with dynamic increasing the BMC after 6 months and passive after 9 months. However, the BMC increase within the dynamic standing intervention reaches statistical significance within Regions 6 through 9, whereas the passive standing only reaches significance in Region 9. This suggests that dynamic standing has a greater impact than the passive standing intervention. Based upon the calculated means, it appears that dynamic standing increases BMC from baseline on the order of 13% (+-5%) in the dynamic standing intervention and 8% (+-5%) in the passive standing intervention over 15 months. These increases are similar to the differences in BMC found between active and inactive children (Bailey et al. 1999). As the increases within the Bailey et al.

study were over a six year span, this study's ability to reach similar magnitudes of increase in 15 months further suggests the potential of a plateau for the impact of the intervention.

The trends of each intervention on the ROI area of the bone show no consistent trends within either standing intervention, nor do they show differences in the magnitude of percent change consistently. This suggests that the type of standing intervention is not the significant factor. As the trends are not consistent, the natural growth of the subject while participating in the study could be the potential factor. With the small population size in this study, as one or more subjects in each group experiences a growth spurt, the mean percent change in area increases. Since growth spurts within each group would be inconsistent, this explains why the trends seen within the ROI area in this study are inconsistent. However, within the confines of this study, it cannot be determined with certainty that the natural growth of the subjects is the significant factor. In future studies, longitudinal data should be collected on the anatomical growth of the femur at each time period to determine if there is any correlation. If growth spurts were present during the significant increases in ROI area, the increases could be attributed to the natural growth of the child.

One important observation in the statistical analyses of the full fifteen month study is the difference in the levels which reach significance between the Henderson et al. (2002) ROIs and the one centimeter ROIs. As discussed briefly in Chapter 3, the two sets of ROIs do not cover the same regions or ratio of the femur within each subject. The Henderson et al. ROIs are anatomically based, with the height of the ROI dependent upon the width of the mid-shaft of the femur, whereas the one centimeter ROIs are set. This

leads to the Henderson et al. ROIs covering a range of six to nine centimeters in the distal femur between subjects (two to three centimeters per ROI), while the one centimeter ROIs expand the distal eight centimeters of the femur in all subjects. One limitation of the two sets of ROIs expanding different total areas of the femur is that the direct outcome measures and statistical significance between the sets cannot be compared numerically. However, the difference in the significant increases found within each set of ROIs can be compared to suggest underlying trends and the impact of growth in the subjects during the study. The analysis of data in this study suggests, as anticipated, that the one centimeter ROIs can provide insight into the trends occurring within the bone that the Henderson et al. ROIs are not able to.

One current unresolved issue in longitudinal studies investigating the effect of mechanical loading on BMD, BMC and area in children with a DXA densitometer is the direct impact growth has on the outcome measures. This remains unresolved in this study. In children, 70% of femur growth occurs at the distal growth plate. During the 15-month duration of this study, the subjects experienced 2 to 4 centimeters of growth in total height. Using anthropometric data (Winter 1990) to estimate the equivalent growth of the femur (total height change*0.25), the femur was calculated to undergo 0.5 to 1 centimeter of longitudinal growth throughout the duration of the study. As 70% of this growth occurred at the distal growth plate, the longitudinal growth of the femur within the ROIs in this study would be 0.35 to 0.7 centimeters. Based upon this magnitude, the impact growth has on the measurements of BMD, BMC and ROI area is a concern. In the one centimeter ROIs, this magnitude of growth could be responsible for temporally shifting the bone proximally almost one full ROI between 0- and 15-months. Therefore,

the bone investigated in ROI 2 in month 0 would be in ROI 3 in month 15, ROI 3 would be in ROI 4 and so on.

The Henderson et al. ROIs may account for some of this growth as when the femur grows longitudinally, it also grows in width. An increase in width would thereby lead to an increased height in the ROI and the Henderson et al. ROIs would then cover similar ratios of the whole bone length throughout the duration of the study. While the Henderson et al. ROIs may account for a degree of longitudinal growth, it was observed in the scans in this study that the ROIs could be masking trends. One reason for this anomaly could be the relatively large ratio of the femur length which the ROIs cover, coupled with the trends suggesting the standing interventions have a greater impact on cortical bone than trabecular within the duration of this study.

One limitation in this study, as briefly discussed above, is the lack of anatomical estimations of the growth of the femur throughout the study. However, this limitation should not be considered detrimental to the results and conclusions of the study. The first observation is that the rate of growth between the subjects in the passive standers is not significantly different than those in dynamic standers. Therefore, growth should have the same impact on each group, but a significant increase in BMD and BMC is determined in dynamic standing versus passive standing despite the potential growth in each group. The trends in Figure 5.1 (identical figure as Figure 3.10) also suggest growth does not invalidate the eight one centimeter ROIs as the trends remain constant throughout the duration of the study. In each time period, the trends show a decrease in BMD in ROI 3 with a steady increase to ROI 7 and a plateau at ROI 8. The three Henderson et al. ROIs

in Figure 5.2 do not illustrate the expected trends, suggesting that the larger area of the three ROIs mask the trends in BMD.

As the trends in Figure 5.1 remain the same throughout the 15-months, any potential impact of growth would remain consistent throughout the study and therefore growth becomes a constant confounding factor. The significant increase in dynamic standing versus passive standing then occurs despite growth. In addition, the trends suggest the spatial location of the area of growth in the femur remains constant in relation to the location of the growth plate. Therefore, placing ROIs based upon a constant distance from the growth plate (as in the one centimeter ROIs) throughout the study instead of those which move proximally with growth (as in the Henderson et al. ROIs) would be more appropriate to determine the impact of each standing intervention in the area of prevalence for femur fractures.

Figure 5.1 also suggests that if growth does have a significant impact on BMD, this study would underestimate the significance. For instance, if ROI 3 at 12 months (in purple) is considered, this study compares ROI 3 at 0 months with ROI 3 at 15 months and determines there to be an increase. If growth were accounted for, then ROI 3 at 0 months should be compared to ROI 4 at 15 months and the increase in BMD would be even greater. This study would be considering an increase of lesser magnitude and the significance of the interventions would be greater if growth were accounted for, thereby strengthening the significance found within this study.

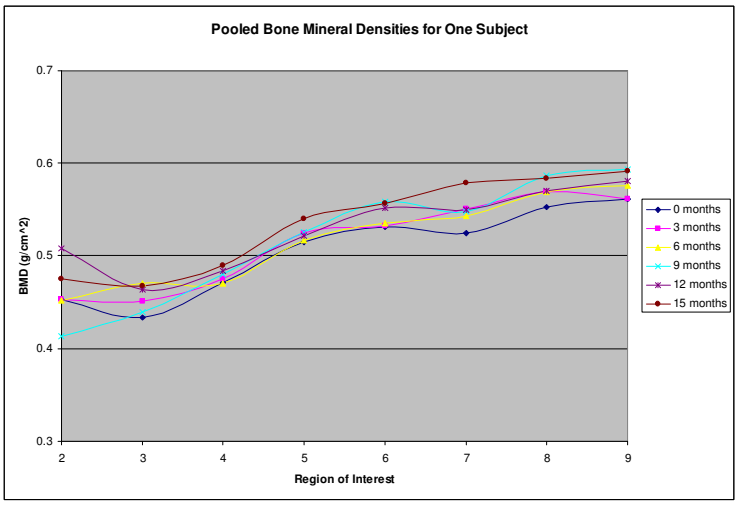

Figure 5.1 Pooled bone mineral densities for one representative subject (one cm ROIs). ROI 2 is located in the trabecular bone immediately above the distal growth plate with ROIs 3 through 9 aligned proximally into the mid-shaft of the femur. As expected, the BMD decreases in Region 3, where the distal femoral head is beginning to decrease in cross-sectional diameter (or 'neck in') and then increases until it nears a plateau in the mid-shaft area of Regions 8 and 9.

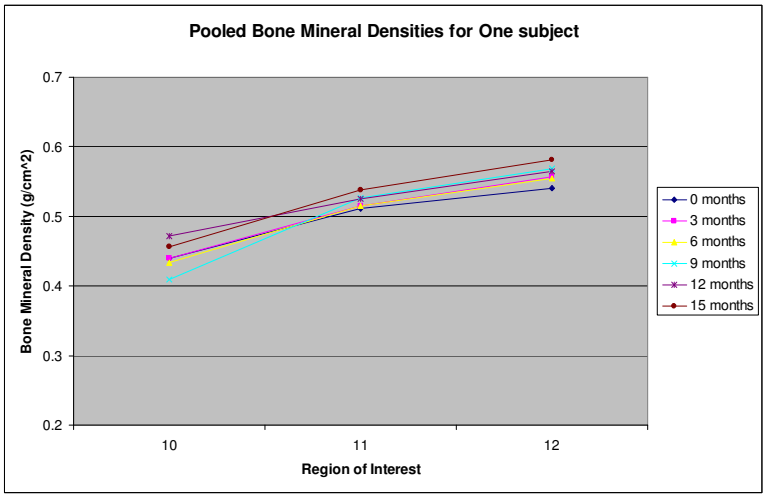

Figure 5.2 Pooled bone mineral densities for one representative subject (3 ROIs). The relative size of the three Henderson et al. (2002) ROIs mask the trends expected in bone mineral density in the distal femur. When compared to the trends in the one centimeter ROIs in Figure 5.1, it can be seen that the one centimeter ROIs more appropriately represent the trends of BMD in the region of fracture.

The increases in the BMD, BMC and ROI area in this study may at first appear to be conservative for 15 months of intervention. However, when considering the limitations of the study and the potential for confounding factors, the percent changes that were observed are significant as they occur without direct control of all factors in the environment. The changes are also significant as they are occurring within the fracture region in the distal femur of these children. While one aim of this study was to increase the population size, the realities of research in a clinical setting prevented the desired population size from being achieved for the full duration of the study. A comparison of the levels of significance within the first six months, which included 13 subjects, versus the full 15 months, which included only 9 subjects, demonstrates that by increasing the population size by 4 children, the power of the study is increased. Another reality of the study was that all factors within the subject's daily life could not be controlled without significant disruptions. Therefore, uncontrolled factors such as diet, activities outside of school and the growth in the children (as previously discussed in detail above), could have a detrimental effect. In spite of the potential impact these confounding factors could have on the study results, a measurable improvement in BMD was still achieved. This is highly significant as a secondary goal of this study was to incorporate the standing interventions into the lives of the subjects without disruption. The success of doing so and still achieving positive results suggests great potential for the standing interventions.

The potential benefit of the dynamic standing intervention is also promising when considering the conservative nature of the dynamic weight-bearing in this study. With the increased risk of fracture in these children and the significant amount of body weight support the body of the stander provides when the children are strapped in, the forces

applied during the dynamic standing were limited to a minimum of about 5% total body weight and maximum of 25%, with no period analogous to single stance. In gentle walking, single stance occurs and the forces reciprocate between 0 to 100% of total body weight. The difference of body weight shift of our forces is expected to have a significant impact, as demonstrated through the comparison of the dynamic and passive forces applied in this study. In ideal passive standing, the weight bearing would be continuous, 50% total body weight on either leg for the duration of the studies. However, in reality, the standers support a large amount of whole body weight and subjects shift their weight with the true range of force encompassing 17 to 20% of total body weight, so that the passive standing intervention in this study is mildly dynamic. Considering the magnitude of difference in the ranges of total body weight, the dynamic standing intervention within this study could potentially have an even greater impact on BMD, BMC and ROI area in the future if the forces are increased to mimic the true forces experienced during gentle walking.

While statistical significance has been determined within the factors associated with BMD, BMC and ROI area, the clinical significance is still unknown. Statistical and clinical significance have different definitions. In adults, the clinical measurement for significance is the T-score for DXA. However, these scores are based on data collection in adult populations and are not suggested to be used in pediatric populations. Until a normalized database can be established for the population being considered in this study, a study of longer duration would have to be completed.

Insurance companies are increasingly denying reimbursement of the passive standers, often citing, “the clinical evidence in published peer-reviewed medical literature

is insufficient to show that a stander is an effective treatment for neuromuscular disorders and potential medical conditions" (insurance company to remain anonymous, but quote retrieved from denial received by Sheila Blochlinger, April 15, 2010). The small number of subjects in the available literature and the mixed results across the field fuels the insurance companies' claims. Therefore, this study aimed at filling the current gaps in the medical literature by investigating not only the impact of passive standing on BMD, but also the impact of a novel dynamic stander designed specifically for this study. The dynamic standing intervention did increase BMD and BMC and therefore has the potential to decrease the number of fractures, the pain the children experience and the further immobilization associated with fractures. The results of this study give credence to the necessity of standing interventions and the need for reimbursement in order to improve the quality of life of these children.

5.2 Conclusions

The principle hypothesis in this study was that reciprocal loading applied during dynamic standing increases the bone mineral density (BMD) of the distal femur at a greater rate than the relatively static loading applied in passive standing. A 15-month comparison between results with dynamic and passive standing interventions showed that dynamic standing produces increases in BMD and BMC greater than those demonstrated in passive standing. As previous literature suggests, it is concluded that passive standing appears to maintain BMD.

In addition, this study suggests that a minimum of six months of intervention is required before significant changes in bone health parameters within the cortical bone are observed and fifteen months for trabecular bone. Another observation from this study is

the impact passive and dynamic standing interventions have on BMC and area do appear to be more significant in the cortical bone in the dynamic standing intervention.

The bone diameter, as represented by the ROI area, in both intervention groups did increase throughout the duration of the study. However, the increase in area was not consistent. Therefore, the increase in area is most likely associated with the natural growth and not the intervention. In future studies, estimates of the anatomical growth of the femur should be collected throughout the study to confirm if the increase in cross-sectional area does correspond to an increase in the length of the femur or if the increase is associated with mechanical loading in the upright position independent of loading parameters.

After the commencement of this study, one subject began to ambulate independently. While the subject was still continued in this study, the data was not analyzed with the previous data summarized in Chapter 5. As a single case, no significant outcomes can be concluded from this subject. However, analysis of the data did reveal approximately 15% greater increases in BMD in this subject over the other subjects in the dynamic standing intervention. As the fragility of the subjects was a concern in this study, conservative forces were applied (alternating between 20 to 80% of body weight). The greater magnitude of increase in the ambulating subject suggests that in future studies, the potential benefit to bone health would be greater if the dynamic standing were applied conservatively at the beginning of the study to ensure tolerance, but then gradually increased to simulate the true forces experienced in ambulation.

5.3 Future Work and Considerations

While a pilot study and necessary prototype modifications were completed prior to the implementation of the dynamic stander in the clinical setting for this 15-month study, additional design modifications continued to be revealed to further improve its incorporation into the clinical setting. The use of a compressor is not ideal for the clinical setting as space is not readily available in the classrooms and moving the compressor between classrooms becomes cumbersome on the staff. Therefore, the implementation of electrical actuators into the design of the footplates is suggested for future prototypes. However, the primary design concepts of creating minimal noise and maintaining a sterile environment, which dictated the use of pneumatic actuators in the original prototype, should be considered when choosing an electrical actuator.

Reducing the staff and size of the equipment needed to run the dynamic stander would also allow future studies into dynamic standing to be expanded to multiple sites, thereby allowing the potential of greater population sizes. Although this study was able to recruit 14 participants for Phase 1 and ten for the full 15 months, it is still necessary to continue increasing the population size in future studies.

Outcome measures, other than bone mineral density, bone mineral content and diameter, should be considered in future studies as well. Standing has been found to impact heart rate variability, bowel and bladder function, respiratory function, behavior and muscle tone. Outcome measures such as these should be included in the future to further demonstrate the magnitude of the benefits of standing interventions for insurance reimbursement.

Continuing to work with General Electric to incorporate the edge detection algorithms and point-typing thresholds investigated in this study would also aid in increasing the potential population sizes. If the precision of the study could be increased independent of a single technician manually editing the images for analysis, multi-site studies could be conducted and study results could be compared between research groups.

To further investigate whether weight-bearing in the upright position or natural growth is responsible for the increases in BMC and area, future studies should follow a population of non-ambulatory children not participating in any standing interventions and a population of ambulatory children to understand the full spectrum of weight-bearing.

Increased study duration should be considered in future studies. Changes in trabecular bone health have been demonstrated to take more time than those in cortical bone within these standing interventions. Increasing the duration of the study could not only lend insight into the impact on each type of bone, but also demonstrate if the potential benefits of the interventions reach a plateau level.

Later investigations into the impact of the dynamic stander should consider incorporating whole-body vibration as well. Currently, coupling the large forces applied to the long bones during ambulation and the low-magnitude, high-frequency vibrations which mimic the muscle forces is hypothesized to be ideal in stimulating bone health. While this study attempted to first mimic the large forces applied during ambulation to the long bones of immobilized children, later investigations combining the two effects should be considered.

APPENDIX A

MATLAB SOURCE CODE FOR CONTROLLING THE DYNAMIC STANDER AND COLLECTING FORCES WITH LOAD CELLS

The program below will control the actuators, load cells and dynamic aspect of the stander. The user must input the duration of the therapy in minutes, and the weight of the individual in pounds. The specific voltage corresponding to the load cell must be entered as well.

```
%   Dynamic Loading in Standing Therapy.
%   Spring 2007.
%   Created by Megan Damcott.

%%%%%%%%%%%%%%%%%%%%%%%%%%%%%%%%%%%%%%%%%%%%%
%   This program will control the actuators and dynamic aspect of the
%   stander. The user must input the duration of the therapy in minutes,
%   and the weight of the individual in pounds. The specific voltage
%   corresponding to the load cell must be entered as well.
%%%%%%%%%%%%%%%%%%%%%%%%%%%%%%%%%%%%%%%%%%%%%

%%%%%%%%%% GUI Creation %%%%%%%%%%

function varargout = Dynamic_standing(varargin)
% DYNAMIC_STANDING M-file for Dynamic_standing.fig
% DYNAMIC_STANDING, by itself, creates a new DYNAMIC_STANDING or raises the existing
singleton*.
%
% H = DYNAMIC_STANDING returns the handle to a new DYNAMIC_STANDING or the handle to the
existing singleton*.
%
% DYNAMIC_STANDING('CALLBACK',hObject,eventData,handles,...) calls the local function named
CALLBACK in DYNAMIC_STANDING.M with the given input arguments.
%
%DYNAMIC_STANDING('Property','Value',...) creates a new DYNAMIC_STANDING or raises the
existing singleton*.  Starting from the left, property value pairs are applied to the GUI before
Dynamic_standing_OpeningFunction gets called.  An unrecognized property name or invalid value makes
property application
stop.  All inputs are passed to Dynamic_standing_OpeningFcn via varargin.
%
%      *See GUI Options on GUIDE's Tools menu.  Choose "GUI allows only one
%      instance to run (singleton)".
%
% See also: GUIDE, GUIDATA, GUIHANDLES

% Edit the above text to modify the response to help Dynamic_standing
%     Last     Modified     by     GUIDE     v2.5     26-Jul-2007     11:43:23
```

```
% Begin initialization code - DO NOT EDIT
gui_Singleton = 1;
gui_State = struct('gui_Name',       mfilename, ...
                   'gui_Singleton',  gui_Singleton, ...
                   'gui_OpeningFcn', @Dynamic_standing_OpeningFcn, ...
                   'gui_OutputFcn',  @Dynamic_standing_OutputFcn, ...
                   'gui_LayoutFcn',  [] , ...
                   'gui_Callback',   []);
if nargin && ischar(varargin{1})
    gui_State.gui_Callback = str2func(varargin{1});
end

if nargout
    [varargout{1:nargout}] = gui_mainfcn(gui_State, varargin{:});
else
    gui_mainfcn(gui_State, varargin{:});
end
% End initialization code - DO NOT EDIT

% --- Executes just before Dynamic_standing is made visible.
function Dynamic_standing_OpeningFcn(hObject, eventdata, handles, varargin)
% This function has no output args, see OutputFcn.
% hObject    handle to figure
% eventdata  reserved - to be defined in a future version of MATLAB
% handles    structure with handles and user data (see GUIDATA)
% varargin   command line arguments to Dynamic_standing (see VARARGIN)

% Choose default command line output for Dynamic_standing
handles.output = hObject;

% Update handles structure
guidata(hObject, handles);

% UIWAIT makes Dynamic_standing wait for user response (see UIRESUME)
% uiwait(handles.figure1);


% --- Outputs from this function are returned to the command line.
function varargout = Dynamic_standing_OutputFcn(hObject, eventdata, handles)
% varargout  cell array for returning output args (see VARARGOUT);
% hObject    handle to figure
% eventdata  reserved - to be defined in a future version of MATLAB
% handles    structure with handles and user data (see GUIDATA)

% Get default command line output from handles structure
varargout{1} = handles.output;
%%%%%%%%%%%%%%%%%%%%%%%%%%%%%%%%%%%%%%%%%%%%%%%%%%%

%%%%%%%%%% START PUSHBUTTON %%%%%%%%%%%%

% At the press of the Start Pushbutton, the valve program begins running.

% --- Executes on button press in startbutton.
function startbutton_Callback(hObject, eventdata, handles)
% hObject    handle to startbutton (see GCBO)
```

```
% eventdata  reserved - to be defined in a future version of MATLAB
% handles    structure with handles and user data (see GUIDATA)

%   Check to see if serial ports are open and close them if necessary. Also
%   clear any data from the buffers.
% port1=exist('s1','var');    % Signal conditioner for info on right foot.
% if port1==1
%     fclose(s1);
%     delete(s1);
%     clear(s1);
%     pause(1);
% end
% port2=exist('s2','var');    % Signal conditioner for info on left foot.
% if port2==1
%     fclose(s2);
%     delete(s2);
%     clear(s2);
%     pause(1);
% end


%%%%%%%%%%%% LOAD CELL PORT SETTINGS %%%%%%%%%%%%%%
%   Open serial port for signal processor to send right load cell
%   information to the computer.
%
s1=serial('COM1','BaudRate',9600,'DataBits',7,'FlowControl','none','Parity','odd','InputBufferSize',1000000,
'OutputBufferSize',1000000);
% fopen(s1);

%   Open serial port for signal processor to send left load cell
%   information to the computer.
%
s2=serial('COM4','BaudRate',9600,'DataBits',7,'FlowControl','none','Parity','odd','InputBufferSize',100000,'
OutputBufferSize',100000);
% fopen(s2);

%%%%%%%%%%%%%%%%%%%%%%%%%%%%%%%%%%%%%%%%%%%%%


%%%%%%%%%%%% LOAD CELL CALIBRATION DATA %%%%%%%%%%%%
%   Pull weight from edit text box.
    w = get(handles.weight,'String');
    w = str2double(w);

%   Voltage output of right load cell at 100 pounds (in millivolts).
%   (Maximum voltage of load cell under right foot.)
    rmaxvolt = 7.9445;   % Load cell balance 0.0992

%   Voltage output of right load cell at 100 pounds (in millivolts).
%   (Maximum voltage of load cell under left foot.)
    lmaxvolt = 8.1231;    % Load cell balance -0.0419

%   Voltage equal to full body weight of child on right foot.
    rbwvolt = w*rmaxvolt/100;

%   Voltage equal to full body weight of child on left foot.
```

```
   lbwvolt = w*lmaxvolt/100;
%%%%%%%%%%%%%%%%%%%%%%%%%%%%%%%%%%%%%%%%%%%%%


%%%%%%%%%%%%%%% CYCLE TIMING %%%%%%%%%%%%%%%%%

%   Pull session duration from edit text box.
   T = get(handles.sessionduration,'String');
   T = str2double(T);

%   Pull gait cycle time from edit text box.
%     g = get(handles.gaitcycletime,'String');
%     g = str2double(g);
   g = 1.5;

%   Number of cycles per leg calibrated for MATLAB timing to match session
%   timing desired. (Calibrated for 30 minute sessions.)
   cycles = (T*60/(1.925*g))*1.03854775;

%   Multiply by 100 to turn percentages into integer multipliers.
   c = cycles*100;

%   Create digital I/O adapter for actuator control.
   digio = digitalio('parallel','LPT1');
%   Adding lines to the digital I/O adapter. Specify the adapter, the
%   numeric IDs of the hardware lines added, the port number, the
%   direction, and name the lines.
   line=addline(digio,0:7,'Out'); %{'Right_Actuator','Left_Actuator'}
%%%%%%%%%%%%%%%%%%%%%%%%%%%%%%%%%%%%%%%%%%%%%


%%%%%%%%%%%% PARAMETERS %%%%%%%%%%%%%%%%%%%%
%   Parameters of gait cycle in which code based on:
   %   40% of leg's gait cycle is swing.
   %   60% of leg's gait cycle is stance.
      %   Initial 20% of stance is double stance.
      %   Mid 60% of stance is single stance.
      %   Final 20% of stance is double stance.
%%%%%%%%%%%%%%%%%%%%%%%%%%%%%%%%%%%%%%%%%%%%%


%%%%%%%%%%%%%% CONTROL LOOP %%%%%%%%%%%%%%%%%%
%   Loop determining timing of the power and inflation status of the actuators.


%   Loop runs for the number of cycles determined above. Includes reading the current voltage of the load cells.
   i=0;
   tt=[];

%   Converting signal conditioner code of *X01 to binary vector in order to read load cell values.
%     P = '*X01';
   P=[42 88 48 49 13];
%   Create loop to read the load cell data continuously.
   a1=[];  % Empty matrix for recording right load cell data.
   b1=[];  % Empty matrix for recording left load cell data.
```

```
   tp=[];  % Empty matrix for recording time for load cell data.
   tic;

for i=1:1:cycles
   % Determining the time (in seconds) of the beginning of the
   % current cycle.
   time = g*i-g;
   % Incremental time for cycle to run.
   t=0;
   for t = time:0.12*g:time+g
      tcl = t;
   % Loop that controls the actuators based upon the timing of
   % the current cycle. (Line 1 is Right actuator and line 2 is left
   % actuator. 1 means inflation and 0 means deflation of the actuators.)
      if t>time && t<=time+0.1*g
         putvalue(digio,[1 0 0 0 1 0 0 0]); %was 1 for second foot [1 0 0 0 0 0 0 0]
%           pause(0.01*g);
      elseif t>time+0.1*g && t<=time+0.5*g
         putvalue(digio,[1 0 0 0 0 0 0 0]); % [1 0 0 0 0 0 0 0]
%           pause(0.01*g);
      elseif t>time+0.5*g && t<=time+0.6*g
         putvalue(digio,[1 0 0 0 1 0 0 0]); % 1 0 0 0 1 0 0 0
%           pause(0.01*g);
      elseif t>time+0.6*g && t<time+g
         putvalue(digio,[0 0 0 0 1 0 0 0]); % [0 0 0 0 1 0 0 0]
%           pause(0.01*g);
      elseif t==time+g
         putvalue(digio,[0 0 0 0 0 0 0 0]); % [0 0 0 0 1 0 0 0]
      end
   % Loop that reads the load cell data for each foot.
%       for j=tcl
%       fprintf(s1,'%c',P);    % Send command for read to signal processor.
%       while s1.BytesAvailable == 0
%       end
%       a=fscanf(s1,'%c',11);  % Read signal processor signal.
%       fprintf(s2,'%c',P);    % Send command for read to signal processor.
%       while s2.BytesAvailable == 0
%       end
%       b=fscanf(s2,'%c',11);  % Read signal processor signal.
%       a1=[a1;a];             % Matrix containing all data. (Right)
%       b1=[b1;b];             % Matrix containing all data. (Left)
%      Creating a loop that will stop the code if the voltage read by the
%      load cell is greater than the child's full body weight.
%       if  a >= rbwvolt | b >= lbwvolt
%          break
%       end
%       end
      ptoc = toc;
      tp=[tp;ptoc];          % Time matrix.
   end
   putvalue(digio,[0 0 0 0 0 0 0 0]); % Returning both actuators to
                                      % deflated resting position.
   ttoc = toc;
   tt=[tt;ttoc];
end
```

```
% Close signal processor/load cell ports.
% fclose(s1)
% fclose(s2)


% Pull the magnitudes of voltage from the signal processor output.
% (Excluding the *X01 code that is returned with the force from the signal
% processor.)
% xxa=[a1(:,4),a1(:,5),a1(:,6),a1(:,7),a1(:,8),a1(:,9),a1(:,10)];
% xxb=[b1(:,4),b1(:,5),b1(:,6),b1(:,7),b1(:,8),b1(:,9),b1(:,10)];
%
% plp=[];
% prp=[];
% Loop converting the load cell voltage data from characters to numbers to
% allow analysis.
% for i=1:length(xxa)
%     p(i)=str2num(xxa(i,:));
%     pp(i)=str2num(xxb(i,:));
% end
% plp=[plp; p];       % Data for the left foot.
% plpp=plp./(lmaxvolt*100);
% minl=min(plpp)
% maxl=max(plpp)
% prp=[prp; pp];      % Data for the right foot.
% prpp=prp./(rmaxvolt*100);
% minr=min(prpp)
% maxr=max(prpp)
% xa=eval('xxa');     % Evaluating each foot.
% xb=eval('xxb');
% xaplot=xa;          % Right foot vector for plotting.
% xbplot=xb;          % Left foot vector for plotting.
% y=tp/60;            % Time vector for plotting.

% Saving trial for later analysis.
save('Deletetrial');


% Plot load cell data.
% figure(1)
% subplot(2,1,1)
% plot(y,plpp); title('Left foot'); xlabel('Time'); ylabel('Voltage');
% subplot(2,1,2)
% plot(y,prpp); title('Right foot'); xlabel('Time'); ylabel('Voltage');

% Total time of session.
ttt=sum(tt)
%%%%%%%%%%%%%%%%%%%%%%%%%%%%%%%%%%%%%%%%%%%%%


%%%%%%%%% EMERGENCY STOP PUSHBUTTON %%%%%%%%%%%%%
% --- Executes on button press in stopbutton.
function stopbutton_Callback(hObject, eventdata, handles)
% hObject    handle to stopbutton (see GCBO)
% eventdata  reserved - to be defined in a future version of MATLAB
% handles    structure with handles and user data (see GUIDATA)
```

```
%%%%%%%%%%%%%%%%%%%%%%%%%%%%%%%%%%%%%%%%%%%%%%%%
% return


%%%%%%%%%USER CONTROLLED VARIABLES%%%%%%%%%%

%   Calls data entered in the edit text boxes. (Therapist input)


%%%%%%%%%%% SESSION DURATION INPUT %%%%%%%%%%%%%%%%
function sessionduration_Callback(hObject, eventdata, handles)
% hObject    handle to sessionduration (see GCBO)
% eventdata  reserved - to be defined in a future version of MATLAB
% handles    structure with handles and user data (see GUIDATA)

% Hints: get(hObject,'String') returns contents of sessionduration as text
%        str2double(get(hObject,'String')) returns contents of sessionduration as a double


% --- Executes during object creation, after setting all properties.
function sessionduration_CreateFcn(hObject, eventdata, handles)
% hObject    handle to sessionduration (see GCBO)
% eventdata  reserved - to be defined in a future version of MATLAB
% handles    empty - handles not created until after all CreateFcns called

% Hint: edit controls usually have a white background on Windows.
%       See ISPC and COMPUTER.
if ispc && isequal(get(hObject,'BackgroundColor'), get(0,'defaultUicontrolBackgroundColor'))
    set(hObject,'BackgroundColor','white');
end
%%%%%%%%%%%%%%%%%%%%%%%%%%%%%%%%%%%%%%%%%%%%%%%


%%%%%%%%%%%%% SUBJECT WEIGHT INPUT %%%%%%%%%%%%%%%%
function weight_Callback(hObject, eventdata, handles)
% hObject    handle to weight (see GCBO)
% eventdata  reserved - to be defined in a future version of MATLAB
% handles    structure with handles and user data (see GUIDATA)

% Hints: get(hObject,'String') returns contents of weight as text
%        str2double(get(hObject,'String')) returns contents of weight as a double


% --- Executes during object creation, after setting all properties.
function weight_CreateFcn(hObject, eventdata, handles)
% hObject    handle to weight (see GCBO)
% eventdata  reserved - to be defined in a future version of MATLAB
% handles    empty - handles not created until after all CreateFcns called

% Hint: edit controls usually have a white background on Windows.
%       See ISPC and COMPUTER.
if ispc && isequal(get(hObject,'BackgroundColor'), get(0,'defaultUicontrolBackgroundColor'))
    set(hObject,'BackgroundColor','white');
end
%%%%%%%%%%%%%%%%%%%%%%%%%%%%%%%%%%%%%%%%%%%%%%%%
```

APPENDIX B

MODIFIED PEARSON AND ROBINSON EDGE DETECTION ALGORITHM

The program below will import a .jpg image and with user defined threshold levels, determine the bone edges within the image. This is more accurate and reproducible than the current manual point-typing used in the clinical setting.

```
function J = pearson_robinson2(image,q,T1,T2,T3)
% Pearson and Robinson edge detection to detect bone edges in DXA image
% analysis. Uses a 5 x 5 array with a pseudo-Laplacian to detect changes in
% acceleration. Must input image and 3 thresholds to determine the edges of the
% horizontal, vertical and diagonals.
% November 2010
% Megan Damcott

% Load image for analysis.
[ZZ,map] = imread(image);

% Change image to 2D gray scale.
Z = rgb2gray(ZZ);
z = Z;

% Look at all pixel values and if grayscale value is less than 20, set
% pixel value to 0.

% Determine the number of pixels in image.
[r,c]=size(Z);

a=[];
b=[];

% First threshold level set to eliminate noise within the muslce and avoid
% detection of islands in later threshold detections.

for a=(1:1:r)
   for b=(1:1:c)
      if Z(a,b) <= q
         Z(a,b) = 0;
      end
   end
end

% Run the Pearson, Robinson edge detection algorithm on the image.
% Taken from: Pearson, Don and John Robinson. (1985) Visual Communication at
% Very Low Data Rates. Proceedings of the IEEE, 73:4, April 1985.

% Draw 5 x 5 matrices, omitting the first and last two rows and columns as
% need two pixels before and two pixels after each pixel of interest to
complete edge detection algorithm.
```

```
x=[];
y=[];
i=0; % Set horizontal indices for loop.
j=0; % Set vertical indices for loop.
vertedge=[];
horizedge=[];
diaglredge=[];
diagrledge=[];

for i=(3:1:r-2); % Loop through each row ommitting the first and last two rows.
   for j=(3:1:c-2); % Loop through each column of each row ommitting the first and last two columns.
      A=Z(i-2,j-2);
      B=Z(i-2,j-1);
      C=Z(i-2,j);
      D=Z(i-2,j+1);
      E=Z(i-2,j+2);
      F=Z(i-1,j-2);
      G=Z(i-1,j-1);
      H=Z(i-1,j);
      I=Z(i-1,j+1);
      J=Z(i-1,j+2);
      K=Z(i,j-2);
      L=Z(i,j-1);
      M=Z(i,j);
      N=Z(i,j+1);
      O=Z(i,j+2);
      P=Z(i+1,j-2);
      Q=Z(i+1,j-1);
      R=Z(i+1,j);
      S=Z(i+1,j+1);
      T=Z(i+1,j+2);
      U=Z(i+2,j-2);
      V=Z(i+2,j-1);
      W=Z(i+2,j);
      X=Z(i+2,j+1);
      Y=Z(i+2,j+2);
      HN=(H+N)/2;
      BH=(B+H)/2;
      NT=(N+T)/2;
      FL=(F+L)/2;
      LR=(L+R)/2;
      RX=(R+X)/2;
      DH=(H+D)/2;
      HL=(L+H)/2;
      LP=(L+P)/2;
      JN=(J+N)/2;
      NR=(N+R)/2;
      RV=(R+V)/2;
      % Look for vertical edge using second and third threshold levels.
      if ((L-M>T1) || (N-M>T1));
         if  ((F+K+P+J+O+T-2*(H+M+R))>T2)  &&  (G+L+Q+I+N+S-2*(H+M+R))>(F+K+P+H+M+R-
2*(G+L+Q)) && (G+L+Q+I+N+S-2*(H+M+R)>(H+M+R+J+O+T-2*(I+N+S)));
            edge1=[i,j];
            vertedge=[vertedge;edge1];
         end
```

```
      end
      % Look for horizontal edge using second and third threshold levels.
      if((H-M>T1) || (R-M>T1));
         if  ((D+C+B+X+W+V-2*(N+M+L))>T2)  &&  (I+H+G+S+R+Q-2*(N+M+L))>(D+C+B+N+M+L-
2*(I+H+G)) && (I+H+G+S+R+Q-2*(N+M+L)>(N+M+L+X+W+V-2*(S+R+Q)));
            edge2=[i,j];
            horizedge=[horizedge;edge2];
         end
      end
      % Look for diagonal 1 (Upper left to lower right) using second and fourth threshold levels.
      if((HN-M>T1) || (LR-M>T1));
         if          ((K+Q+W+C+I+O-2*(G+M+S))>T3)          &&          (RX+LR+FL+BH+HN+NT-
2*(G+M+S))>(K+Q+W+G+M+S-2*(FL+LR+RX))          &&          (FL+LR+RX+BH+HN+NT-
2*(G+M+S)>(G+M+S+C+I+O-2*(BH+HN+NT)));
            edge3=[i,j];
            diaglredge=[diaglredge;edge3];
         end
      end
       % Look for diagonal 2 (Upper right to lower left)using second and fourth threshold levels.
      if((HL-M>T1) || (NR-M>T1));
         if          ((C+G+K+O+S+W-2*(I+M+Q))>T3)          &&          (DH+HL+LP+JN+NR+RV-
2*(I+M+Q))>(C+G+K+I+M+Q-2*(DH+HL+LP))          &&          (DH+HL+LP+JN+NR+RV-
2*(I+M+Q)>(I+M+Q+O+S+W-2*(JN+NR+RV)));
            edge4=[i,j];
            diagrledge=[diagrledge;edge4];
         end
      end
   end
end

vertedge;
horizedge;
diaglredge;
diagrledge;

% Show image and plot the edges detected on image.
J = [vertedge(:,2),vertedge(:,1);
   horizedge(:,2),horizedge(:,1);
   diaglredge(:,2),diaglredge(:,1);
   diagrledge(:,2),diagrledge(:,1)];


figure(1)
imshow(z)
% set(gca,'Units','centimeters')
% set(gca,'Position', [1.9247    1.2214     5.0    15.35])
% imshow(z)
hold on
plot(vertedge(:,2),vertedge(:,1),'y.','MarkerSize',2)
plot(horizedge(:,2),horizedge(:,1),'y.','MarkerSize',2)
plot(diaglredge(:,2),diaglredge(:,1),'y.','MarkerSize',2)
plot(diagrledge(:,2),diagrledge(:,1),'y.','MarkerSize',2)

% saveas(gca,'Pic.jpg')
```

REFERENCES

Bailey, D., Mckay, H., Mirwald, R., Crocker, P., and Faulkner, R. (1999) A Six-Year Longitudinal Study of the Relationship of Physical Activity to Bone Mineral Accrual in Growing Children: The University of Saskatchewan Bone Mineral Accrual Study. *Journal of Bone and Mineral Research, 14:10,* 1671-1679.

Bass, S., Pearce, G., Bradney, M., Hendrich, E., Delmas, P., Harding, A., and Seeman, E. (1998) Exercise Before Puberty May Confer Residual Benefits in Bone Density in Adulthood: Studies in Active Prepubertal and Retired Female Gymnasts. *Journal of Bone and Mineral Research 13:3,* 500-507.

Bloomfield, S.A., Mysiw, W.J., Jackson, R.D. (1996) Bone Mass and Endocrine Adaptations to Training in Spinal Cord Injured Individuals. *Bone, 19:1,* 61-68.

Bonnick, S., Johnston, C., Kleerekoper, M., Lindsay, R., Miller, P., Sherwood, L., Siris, E. (2001). Importance of Precision in Bone Density Measurements. *Journal of Clinical Densitometry, 4:2:* 105-110.

Caulton, JM., Ward, KA., Alsop, CW., Dunn, G., Adams, JE., Mughal, MZ. (2004) A randomised controlled trial of standing programme on bone mineral density in non-ambulant children with cerebral palsy. *Archives of Disease in Childhood, 89,* 131-135

Chad, K., Bailey, D., McKay, H., Zello, G., and Snyder, R. (1999) The effect of a weight-bearing physical activity program on bone mineral content and estimated volumetric density in children with spastic cerebral palsy. *Journal of Pediatrics, 135,* 115-117.

Damcott, M. (2011) The Effect of Dynamic Standing on the Bone Mineral Density of Non-Ambulatory Children: A Pilot Study. Master's Thesis, New Jersey Institute of Technology.

Fewtrell, MS. (2003). Bone densitometry in children assessed by dual x ray absoptiometry: uses and pitfalls. *Archives of Disease in Childhood, 88,* 795-798.

Flinn, E. (2002). Subtle shake-up in bone-loss research. *American Institutes of Aeronautics and Astronautics, Inc. Engineering Notebook,* 16.

Frost, H. (2003). Bone's Mechanostat: A 2003 Update. *The Anatomical Record Part A, 275A,* 1081-1101.

Frost, H. (2004). A 2003 Update on Bone Physiology and Wolff's Law for Clinicians. *Angle Orthodontist, 74:1*, 3-15.

Gilsanz, V., Wren, T., Sanchez, M., Dorey, F., Judex, S. and Rubin, C. (2006) Low-Level, High-Frequency Mechanical Signals Enhance Musculoskeletal Development of Young Women With Low BMD. *Journal of Bone and Mineral Research, 21:9,* 1464-1474.

Gordon, C., Bachrach, L., Carpenter, T., Crabtree, N., Fuleihan, GE., Kutilek, S., Lorenc, R., Tosi, L., Ward, K., Ward, L. Kalkwarf, H. (2008) Dual Energy X-ray Absorptiometery Interpretation and Reporting in Children and Adolexcents: The 2007 ISCD Pediatric Official Positions. *Journal of Clinical Densitometry: Assessment of Skeletal Health, 11:1,* 43-58.

Goulding, A., Gold, E., Cannan, R., Williams, S., Lewis-Barned, N. (1996) Changing Femoral Geometry in Growing Girls: A Cross-Sectional DEXA Study. *Bone, 19:* 645-649.

Gudjonsdottir, B., and Mercer, V. (2002a) A Motorized Dynamic Stander. *Pediatric Physical Therapy, 14,* 49-51.

Gudjonsdottir, B., and Mercer, V. (2002b) Effects of a Dynamic Stander Versus a Static Prone Stander on Bone Mineral Density and Behavior in Four Children with Severe Cerebral Palsy. *Pediatric Physical Therapy, 14,* 38-46.

Harcke, HT, Taylor, A, Bachrach, S, Miller, F, Henderson, RC. (1998). Lateral femoral scan: an alternative method for assessing bone mineral density in children with cerebral palsy. *Pediatric Radiology, 28,* 241-246.

Henderson, R., Lark, R., Newman, J., Kecskemthy, H., Fung, E., Renner, J., Harcke, H. (2002). Pediatric Reference Data for Dual X-Ray Absorptiometric Measures of Normal Bone Density in the Distal Femur. *American Journal of Roentgenology, 178,* 439-443.

Henderson, R., Gilbert, S., Clement, M., Abbas, A., Worley, G., Stevenson, R. (2005) Altered skeletal maturation in moderate to severe cerebral palsy. *Developmental Medicine and Child Neurology, 47,* 229-236.

Ko, C., Tse, P., Chan, A. (2006) Risk factors of long bone fractures in non-ambulatory cerebral palsy children. *Hong Kong Medical Journal, 12:*426-431.

Lanyon, L, Rubin, C. (1984) Static vs dynamic loads as an influence on bone remodeling. *Journal of Biomechanics, 17*, 897-905.

Leet, A., Shirley, E., Barker, C., Launay, F., Sponseller, P. (2009) Treatment of femur fractures in children with cerebral palsy. *Journal of Children's Orthopaedics, 3,* 253-258.

Martin, R., Burr, D, and Sharkey, N. (1998). *Skeletal Tissue Mechanics.* New York: Springer-Verlag.

Marguiles, L., Horlick, M., Thorton, J., Wang, J., Ioannidou, E., Heymsfield, S. (2005) Reproducibility of Pediatric Whole Body Bone and Body Composition Measures by Dual-Energy X-Ray Absorptiometry Using the GE Lunar Prodigy. *Journal of Clinical Densitometry, 8:3:* 298-304.

National Cancer Institute (2008a). *Anatomy and Physiology Module.* Retrieved August 15, 2008 from http://training.seer.cancer.gov/module_anatomy/unit3_4_bone_classification.html

National Cancer Institute (2008b). *Anatomy and Physiology Module.* Retrieved August 15, 2008 from http://training.seer.cancer.gov/module_anatomy/unit3_4_bone_tissue.html.

Pearson, DE. and Robinson, JA. (1985). Visual Communication at Very Low Data Rates. *Proceedings of the IEEE, 73:4:April,* 795-812.

Pearson, O., Lieberman, D. (2004) The Aging of Wolff's "Law": Ontogeny and Responses to Mechanical Loading in Cortical Bone. *Yearbook of Physical Anthropology, 47:* 63-99.

Pietrobelli, A., Formica, C., Wang, Z., Heymsfield, S. (1996) Dual-energy X-ray absorptiometry body composition model: review of physical concepts. *American Journal of Physiology, 271,* E491-551.

Rubin, C, Li, C, Syn, Y, Fritton, C, McLeod, K. (1995) Non-invasive stimulation of trabecular bone formation via low magnitude, high frequency strain. *41st Orthopedic Research Society, 20*, 548.

Rubin, C, Turner, S, Bain, S, Mallinckrodt, C, McLeod, K. (2001a) Low mechanical signals strengthen long bones. *Nature, 412,* 603-604.

Rubin, C, Xu, G, Judex, S. (2001b) The anabolic activity of bone tissue, suppressed by disuse, is normalized by brief exposure to extremely low-magnitude mechanical stimuli. *The FASEB Journal, 15,* 2225-2229.

Rubin, C, Turner, S, Muller, R, Mittra, E, McLeod, K, Lin, W, Qin, Y. (2002a) Quantity and quality of trabecular bone in the femur are enhanced by a strongly anabolic, noninvasive mechanical intervention. *Journal of Bone and Mineral Research, 17,* 349-357.

Rubin, C, Turner, S, Mallinckrodt, C, Jerome, C, McLeod, K, Bain, S. (2002b) Mechanical strain, induced noninvasively in the high-frequency domain, is anabolic to cancellous bone, but not cortical bone. *Bone, 30,* 445-452.

Rubin, C., Recker, R., Cullen, D., Ryaby, J., McCabe, J., and McLeod, K. (2004) Prevention of Postmenopausal Bone Loss by a Low-Magnitude, High-Frequency Mechanical Stimuli: A Clinical Trial Assessing Compliance, Efficacy and Safety. *Journal of Bone and Mineral Research, 19:3,* 343-351.

Specker, B. and Schoenau, E. (2005). Quantitative Bone Analysis in Children: Current Methods and Recommendations. *Journal of Pediatrics, 146,* 726-731.

Surgeon General. (2004) Bone Health and Osteoporosis: A Report of the Surgeon General. *Office of the Surgeon General, U.S. Department of Health and Human Services.*

Verschueren, S., Roelants, M, Delecluse, C., Swinnen, S., Vanderschueren, D., Boonen, S. (2004) Effect of a 6-Month Whole Body Vibration Training on Hip Density, Muscle Strength, and Postural Control in Postmenopausal Women: A Randomized Controlled Pilot Study. *Journal of Bone and Mineral Research, 19:3,* 352-359.

Ward, K., Alsop, C., Caulton, J., Rubin, C., Adams, J., Mughal, Z. (2004) Low Magnitude Mechanical Loading is Ostogenic in Children with Disabling Conditions. *Journal of Bone and Mineral Research, 19:3,* 360-368.

Winters, David. (1990). Biomechanics and Motor Control of Human Movement. 2nd ed. *John Wiley and Sons, Inc, New York.*

Wren, T., Lee, D., Hara, R., Rehtlefsen, S., Kay, R., Dorey, F., Gilsanz, V. (2010) Effect of High-frequency, Low-magnitude Vibration on Bone and Muscle in Children With Cerebral Palsy. *Journal of Pediatric Orthopedics, 30,* 732-738.